Lawrence Berkeley National Laboratory

Recent Work

Title

COUPLING EFFICIENCY OF WAVEGUIDE LASER RESONATORS FORMED BY FLAT MIRRORS: ANALYSIS AND EXPERIMENT

Permalink

https://escholarship.org/uc/item/3qt7q50z

Authors

Gerlach, R.
Wei, D.
Amer, N.M.

Publication Date

1983-11-01

Lawrence Berkeley Laboratory

UNIVERSITY OF CALIFORNIA

APPLIED SCIENCE DIVISION
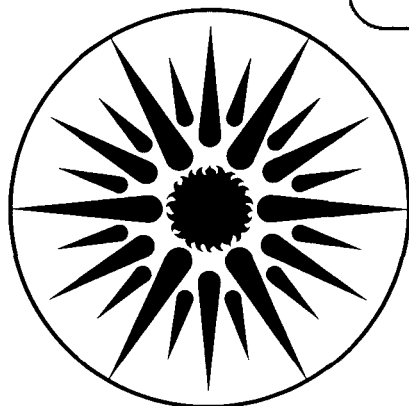
COUPLING EFFICIENCY OF WAVEGUIDE LASER RESONATORS
FORMED BY FLAT MIRRORS: ANALYSIS AND EXPERIMENT

R. Gerlach, D. Wei, and N.M. Amer

November 1983

**APPLIED SCIENCE
DIVISION**

DISCLAIMER

COUPLING EFFICIENCY OF WAVEGUIDE LASER RESONATORS FORMED

BY FLAT MIRRORS: ANALYSIS AND EXPERIMENT

Robert Gerlach, Dianyuan Wei* and Nabil M. Amer

Applied Physics and Laser Spectroscopy Group
Lawrence Berkeley Laboratory
University of California
Berkeley, CA   94720
USA

---

* Visiting scholar from Beijing Vacuum Electron Devices Research Institute, Beijing, China

COUPLING EFFICIENCY OF WAVEGUIDE LASER RESONATORS FORMED

BY FLAT MIRRORS: ANALYSIS AND EXPERIMENT

ABSTRACT

We present a new and more efficient method of calculating the

losses of a waveguide laser resonator consisting of a hollow circular

dielectric waveguide and flat mirrors, taking into account the effects

of waveguide modes up to order HE_{13}. Both symmetric and asymmetric cav-

ities are considered. We show that low cavity losses, only slightly

exceeding the HE_{11} waveguiding losses, are predicted to be possible for

much larger mirror distances than had previously been suspected, pro-

vided that an optimum total cavity length is chosen. The low losses

arise when the HE_{11} and HE_{12} modes emerge from the guide with relative

amplitudes and phases such that the returning diffraction patterns

interfere to produce a narrow beam with low aperture losses. The

theoretical predictions were checked experimentally for CO_2 lasers hav-

ing various waveguide dimensions. Good qualitative agreement was found,

but the optimum total cavity lengths were typically 3-5% longer than

predicted. Possible explanations of this discrepancy are discussed. We

also predicted and experimentally verified that variations of the cavity

length over a few centimeters can exert a coarse wavelength selectivity

sufficient to determine the band and branch on which a CO_2 laser oscil-

lates; conversely, that for a grating tuned laser, the cavity length

must be varied by a similar amount as the wavelength is tuned in order

to maintain low cavity losses over the entire wavelength range.

I. Introduction

Waveguide lasers are generally operated in either of two types of cavity configurations. In the first, two flat mirrors are placed as close as possible to the ends of the waveguide, while the second configuration uses short radius of curvature concave mirrors placed some distance from the ends of the waveguide to refocus the diverging diffracted beam into the ends of the waveguide [1].

Typical radii of curvature for the concave mirrors used for waveguide CO_2 lasers are in the 10-40 cm range, which are not commonly available, and must be custom made. Flat mirrors have the advantage of ready availability and lower cost, but may result in large parasitic cavity losses if the laser structure prohibits placing the mirrors close to the ends of the waveguide, as is frequently the case with lasers having Brewster angle windows. According to theoretical models in which only the lowest-loss HE_{11} mode is assumed to propagate in the waveguide [2], the losses should increase monotonically as the 3/2 power of mirror distance as the flat mirrors are moved away from the ends of the waveguide [3].

A first hint that efficient resonator geometries might be achieved with flat mirrors placed at greater distances was provided by the experiment of Jensen and Tobin [4]. They observed that as a flat mirror was moved away, power at first decreased, but rose to a secondary, unexplained peak when the mirror was a large distance from the waveguide.

Further evidence of this possibility appeared when we made measurements of output power as a function of the mirror distances d_1 and d_2 for a CO_2 waveguide laser of a type we have described previously [5], operated in the flat-mirror cavity configuration shown in Figure 1a. The measurements, pre-

sented in Figure 2, indicate that as one of the mirror distances, d_2, is varied at constant d_1, a peak in power is observed for a distance many centimeters from the waveguide. Furthermore, as the other distance, d_1, is increased, the value of d_2 at which the peak occurs decreases. It was a desire to understand this behavior that motivated this study.

Such an understanding requires the assumption that two or more modes propagate simultaneously in the waveguide. The waveguide modes calculated by Marcatili and Schmeltzer [6] are not eigenfunctions of the cavity as a whole, since diffraction in the free space region produces a mixing of the modes. In the model in which only a single mode propagates in the waveguide [2], the coupling losses at the two ends of the cavity are independent of one another, and increase monotonically with the mirror distances, and hence cannot explain the data of Figure 2. Detailed numerical analyses of waveguide resonators using multiple waveguide modes have been developed [3,7,8], but have not been applied to the case of resonators having flat mirrors at significant distances from the ends of the waveguide. A somewhat more qualitative approach which gives some intuitive insight has been developed [9] and applied to CO_2 waveguide lasers [10], but still no application to flat-mirror resonators has been made.

In this paper we demonstrate that efficient low-loss waveguide laser resonators having flat mirrors far from the ends of the waveguide are possible. We present a method for calculating resonator losses which differs from previous methods in that the number of numerical integrations that must be computed is greatly reduced. We present graphs and simple formulae for selecting an optimum mirror distance for a waveguide of given length and bore diameter, optimum guide length for a given minimum mirror distance and

waveguide bore, and optimum waveguide bore diameter for a laser having a specified free spectral range. We examine the effect of wavelength variation, and show that the resonator configuration can exert a coarse wavelength selectivity without the use of a grating, while in a grating-tuned laser, changes in the total cavity length must accompany tuning of the grating in order to keep the laser in a low-loss configuration.

II. Theory

The resonator geometry with which we will be dealing is shown in Figure 1a. The waveguide, a hollow dielectric tube of radius a and length ℓ, is interposed between two flat mirrors situated at distances d_1 and d_2 from the ends of the tube. We will restrict our consideration to linearly polarized modes having radial symmetry, and neglect the effects of finite mirror aperture, of mirror misalignment, and of the active gain medium within the waveguide. In solving for the modes of this resonator, we will model it as an extended periodic system as shown in Figure 1b, in which the beam emerging from the waveguide in plane A traverses free space regions of lengths $2d_1$ and $2d_2$ and makes two trips through waveguide sections of length ℓ before reaching a plane A' equivalent to the initial plane A. (In the more general resonator geometry in which the mirrors are curved, there would be lenses midway between planes A and B and midway between C and D.) The fields in planes A and A' can be expressed in terms of column vectors $\underline{x}$ and $\underline{x}'$, respectively, whose components are the expansion coefficients of the field in terms of the HE_{1m} hybrid modes of the waveguide [6]. We seek a matrix M which represents the effect of propagating one round trip through the cavity, i.e. from A to A', so that $\underline{x}'=M\underline{x}$. We then find the eigenvalues and eigenvectors of M,

$$M \underline{x}_i = \Lambda_i \underline{x}_i \qquad (1)$$

The round trip loss $\mathcal{L}_i$ for the i'th resonator mode is then given by

$$\mathcal{L}_i = 1 - |\Lambda_i|^2 \qquad (2)$$

Before describing our method, we will briefly review the previous approaches to this problem that have been employed.

The simplest approach, due to Abrams [2], was to assume that the mode propagating in the waveguide was pure HE_{11}. He calculated the coupling losses by expanding the HE_{11} mode in terms of a set of Laguerre-Gaussian modes, allowing those modes to propagate to the mirror and back using the laws of Gaussian beam propagation [11], and calculating the overlap integral of the returning beam with the HE_{11} mode. This model fails to predict the results of our experiment.

Chester and Abrams [7] were the first to consider the effects of higher waveguide modes. They expanded the waveguide modes in terms of a set of free space modes having their beam waist in the exit plane and having a value of w_o/a chosen to make their wavefront radii of curvature match the curvature of the mirror. This method cannot be applied to resonators using flat mirrors because the assumptions that the free space modes have their beam waist in the waveguide aperture plane and that they match the radii of curvature of the mirrors are then contradictory.

Degnan and Hall [3] treated the propagation in the free space region not in terms of an expansion in free space modes, but rather by numerical evaluation of diffraction integrals. They also considered the effect of finite mirror aperture. Abrams and Chester [8] used a similar method except

that they assumed an infinite mirror aperture and treated the propagation from the waveguide to the mirror and back again in terms of a single diffraction integral, again calculated numerically. While the method is capable of handling the case of flat-mirror resonators, neither paper did so except in the context of the pure-HE_{11} model, and it was assumed that that model was always valid for flat-mirror resonators [3].

The above methods are all characterized by the necessity of calculating large numbers of integrals numerically, and generally whenever any cavity parameter is varied (except the waveguide length) it is necessary to recalculate the integrals.

A more qualitative but still useful model was developed by Roullard and Bass [9]. They assumed the field in the waveguide to be a combination of HE_{11} and HE_{12}. A linear combination of these modes with unequal phases has curved phasefronts. They therefore considered the coupling of the beam emerging from the waveguide to a single free space mode, a TEM_{00} mode having its spot size and radius of curvature optimized to match the emerging field. This method has been useful in predicting cavity configurations that would lead to nearly-Gaussian far field patterns, but has not been applied to flat-mirror cavities, nor has the method been used for quantitiative calculation of resonator eigenvalues or losses.

Of the above, our method most closely resembles that of Chester and Abrams [7] insofar as we also expand the field in terms of a set of Laguerre-Gaussian modes having their beam waist in the waveguide exit plane. However, whereas they had to vary w_o/a, and hence recalculate the waveguide to free space mode coupling integrals, whenever they varied their cavity geometry, we were able to greatly reduce the number of numerical integrations

that must be performed by always using the same value of w_o/a and instead

using an analytical transformation between two sets of Laguerre-Gaussian

modes to represent the field returning to the waveguide in terms of modes

having the original spot size w_o and infinite radius of curvature, facili-

tating the transformation back to waveguide modes, as we shall describe

below. As an initial investment one must calculate a relatively small num-

ber of integrals numerically, but then any number of different cavity con-

figurations (different values of d_1, d_2, ℓ, a, or λ) can be analyzed with-

out any further numerical integration. Whereas the method presented by

Chester and Abrams could not be applied to flat-mirror cavities, our method

as presented here is applicable only to flat-mirror cavities, but can be

generalized to curved-mirror cavities, as we plan to describe in a later

paper. We will present an outline of our method below, and further details

in the Appendix.

We seek to express the matrix M representing a complete round trip

through the cavity as a product of matrices, each of which represents either

the effect of propagating through a particular region of the cavity or a

transformation between one set of modes and another. The places where these

various matrices are applied are shown in Figure 1b. Initially, in plane A,

the vector $\underline{x}$ represents the field in terms of waveguide modes. Since the

beam is emerging into a region of free space, we wish to transform to a set

of free-space modes by means of a transformation matrix M_1. Any set of

Laguerre-Gaussian, or TEM_{mQ}, modes, having arbitrary spot size w and radius

of curvature R, constitutes a complete set for representing any radially-

symmetric field in the waveguide exit plane. We have arbitrarily chosen a

set of modes having their beam waist in plane A and having a value of w_o/a

selected according to criteria to be discussed below. The elements of M_1 are determined by numerical integration.

Matrix M_2 is a diagonal matrix representing the relative phase shifts of the various TEM_{m0} modes in propagating a distance $2d_1$ from plane A to plane B.

At this point we deviate from the usual practice of transforming directly back into waveguide modes and instead transform into a different set of TEM modes. The field arriving at plane B is initially represented in terms of a set of TEM modes having an enlarged spot size $w > w_o$ and some finite radius of curvature R. If it were instead represented in terms of TEM modes having their beam waist in the waveguide entrance plane B and having the original spot size w_o, then the transformation to HE_{1m} modes could be performed with the transpose of matrix M_1, whose elements have already been determined. We therefore introduce a matrix M_3 which transforms to the latter set of TEM_{m0} modes, followed by a matrix M_4, the transpose of M_1, which transforms these to waveguide modes. If the matrix elements of M_3 had to be evaluated by numerical integration, then we would have gained nothing by this additional transformation; fortunately, Kogelnik [12] has shown that they can be obtained analytically.

Matrix M_5, which is diagonal, represents the attenuations and relative phase shifts of the HE_{1m} modes in propagating a distance ℓ through the waveguide with propagation constants [6]

$$\gamma_{1m} = k \left[1 - \frac{u_{1m}^2}{2k^2 a^2} \left(1 - \frac{2i\nu_n}{ka} \right) \right] \tag{3}$$

where $k = 2\pi/\lambda$, u_{1m} is the m'th zero of $J_o(u)$, and

$$\nu_n \equiv \frac{\nu^2 + 1}{2(\nu^2 - 1)^{\frac{1}{2}}} \qquad (4)$$

and ν is the complex refractive index of the waveguide material.

In plane C we again apply matrix M_1 to transform to TEM modes. Then matrix M_6 describes the phase shifts in propagating a distance $2d_2$ from C to D in free space, matrix M_7 transforms to a set of TEM modes having spot size w_0 and beam waist in plane D, and matrix M_4 transforms these modes into HE_{1m} modes. A final application of M_5, describing propagation through the waveguide, brings us back to plane A', equivalent to plane A in our periodic scheme. The net round trip matrix is thus given by

$$M = M_5 \, M_4 \, M_7 \, M_6 \, M_1 \, M_5 \, M_4 \, M_3 \, M_2 \, M_1 \qquad (5)$$

Each time d_1 is changed, M_2 and M_3 must be recalculated, while changing d_2 requires recalculating M_6 and M_7. Changing ℓ or ν_n requires recalculating M_5, while changing a or λ requires recalculating all the matrices except M_1 and M_4. Only M_1 and its transpose M_4 need be evaluated by numerical integration, and these need never be recalcuated once evaluated initially.

We note that for the specific case of a symmetric cavity, i.e. one for which $d_1 = d_2$, we have $M_6 = M_2$ and $M_7 = M_3$, and hence

$$M = [M_5 \, M_4 \, M_3 \, M_2 \, M_1]^2 \equiv [M']^2$$

where matrix M' describes the half-cavity. The eigenvalues Λ_i of M are related to the eigenvalues Λ'_i of M' by

$$\Lambda_i = \Lambda'^2_i$$

so that the coupling losses can be found by diagonalizing a much more easily

computed matrix.

The mathematical details of the computation of matrices M_1 through M_7 appear in the Appendix.

Once the matrix M (or M') is determined, we determine its eigenvalues by exact solution of the characteristic polynomial. This is possible because we limited our computations to at most three waveguide modes, so that the polynomial is at most cubic.

Of those portions of the computation that have to be done for each new cavity configuration, most of the time is consumed by the computation of the transformation matrices M_3 and M_7. While the elements of these matrices are algebraic expressions rather than numerical integrals, they are quite complicated, involving hypergeometric functions and factorials. However, if a method like those described by other authors [3,7,8] had been used, at least one set of integrals comparable to those in matrix M_1 would have to be evaluated for each new cavity configuration, and we found that the entire computation excluding calculation of M_1 took typically about one quarter of the time required to calculate M_1. Thus our method results in a fourfold savings in computer time.

The choice of the parameter w_o/a is important and deserves some discussion. In principle, if we were using an infinite number of TEM modes in which to expand the field, the choice of w_o/a would be completely arbitrary, and the solution of Equation (1) would be completely independent of w_o/a. However, since we wish to truncate the expansion with a relatively small number of modes, the value of w_o/a must be chosen to make the expansion converge reasonably rapidly. The following tradeoff is involved: To minimize the truncation error in expanding the field emerging from the waveguide, a

small value of w_o/a is favored. However, a small w_o results in a large divergence for the free space modes, and therefore the returning spot size w will differ greatly from w_o if the mirror distance is significant. This will result in larger trunction errors in the transformation from the set of TEM modes with spot size w back to the set with spot size w_o. Minimizing these truncation errors favors large w_o/a.

We made our choice of w_o/a based on several considerations. First, we observed that as the number of free space modes was increased, with the number of waveguide modes held fixed at two, the most rapid convergence of the solutions occurred for $w_o/a \sim 0.55$, and for this choice six free space modes were adequate for expanding the field. Second, we found that when we used two waveguide modes and six free space modes, the solutions were nearly independent of w_o/a over the range $0.45 < w_o/a < 0.70$. A value near the middle of this interval is desirable.

Based on a physical interpretation to be presented at the end of this section, it makes sense to use a value of w_o/a such that each HE_{1m} waveguide mode couples most of its power into a single free space TEM mode. As is well known [2], the maximum power coupling of 98% from HE_{11} to TEM_{00} occurs at $w_o/a = 0.6435$. This maximum is very broad, however. The maximum HE_{12} to TEM_{10} coupling, 87.6%, occurs at $w_o/a = 0.534$, where the HE_{11} to TEM_{00} coupling is 93.8%. The choice $w_o/a = 0.55$ is a good tradeoff, since it gives 95.1% HE_{11} to TEM_{00} and 87.0% HE_{12} to TEM_{10} coupling. When the HE_{13} mode is included, a smaller value of w_o/a is favored, trading off some HE_{11} to TEM_{00} and HE_{12} to TEM_{10} couping for higher HE_{13} to TEM_{20} coupling; the power coupling coefficients are then 89%, 84%, and 73%, respectively.

Truncation errors for expanding the HE_{1m} modes in terms of six free

space modes with $w_o/a=0.55$ are 0.1% for HE_{11}, 0.8% for HE_{12}, and 4% for HE_{13}. For $w_o/a=0.48$, a more appropriate value for use with three waveguide modes, the errors are 0.07%, 0.45%, and 1.6%, respectively. The higher truncation errors for the higher waveguide modes are tolerable if we are primarily concerned about the lowest loss resonator mode, because most of the power in that mode will be in the HE_{11} waveguide mode. The truncation errors involved in the TEM-TEM mode transformation (matrices M_3 and M_7) were not easily characterized because they depended on both w_o/a and on the mirror distances.

As the above discussion suggests, we used $w_o/a=0.55$ when using two waveguide modes, and a somewhat smaller value, 0.48 or 0.50, when using three modes.

We will now proceed to describe the predictions based on the above model. It will be convenient to define an effective waveguide length

$$\ell' = \ell \left(1 + 2 \text{ Im } \nu_n/ka \right) \qquad (6)$$

This will in general not differ from the actual geometrical length ℓ by more than a few percent, and differences as large as that occur only near material resonances of the waveguide, so in most cases it is a good approximation that $\ell'=\ell$. The waveguide laser resonator using flat mirrors is described entirely in terms of four dimensionless parameters: the mirror distance parameters d_1/ka^2 and d_2/ka^2; the effective waveguide length parameter ℓ'/ka^2, which determines phase shifts in the waveguide; and a waveguide loss parameter $(\text{Re } \nu_n/ka)/(1 + 2 \text{ Im } \nu_n/ka)$. The last-mentioned variable represents the waveguide attenuation per unit increment in ℓ'/ka^2; in propa-

gating a distance $\Delta \ell'/ka^2 = 1$, the amplitude of the HE_{1m} mode is attenuated by a factor of $\exp[-u_{1m}^2(\text{Re } \nu_n/ka)/(1 + 2 \text{ Im } \nu_n/ka)]$. The denominator of this parameter arises because the attenuation in the waveguide depends on the actual length ℓ rather than the effective length ℓ' which determines the phase shifts, so it is necessary to include this factor to obtain the attenuation per unit increment in ℓ'/ka^2. However, the denominator can be assumed to be unity for most purposes, since the effect of this is second order in λ/a. Neglecting the denominator results in an error of only a small percentage of the waveguide losses, which are themselves typically less than 15% per round trip. We therefore use simply Re ν_n/ka as a label in our graphs, although we retained the denominator in our computations, and the reader may interpret the labels as actually being values of $(\text{Re } \nu_n/ka)/(1+2 \text{ Im } \nu_n/ka)$. We present our theoretical predictions in terms of the above four dimensionless parameters, since they will then be more universally useful than predictions in terms of specific dimensional variables found by assuming, for example, specific values of the wavelength, tube radius, and refractive index.

The first phenomenon we tried to understand using our model is the dependence of power on mirror distances exhibited in Figure 2. The fact that a maximum power is observed at some large value of d_2 for a particular fixed value of d_1 indicates that the cavity losses must be a minimum there with respect to variation of d_2 at constant d_1. If d_1 is increased, the value of d_2 at which the minumum loss occurs decreases; the highest overall power is observed when the peak occurs at $d_2 \approx d_1$. In Figure 3a we present a set of loss contours in the d_2/ka^2 vs. d_1/ka^2 plane. These were calculated for

$\ell'/ka^2 = 0.35$ and Re $\nu_n/ka = 0.002$, and two waveguide modes were used in the calculation. While the overall minimum loss of 2.04% occurs at $d_1 = d_2 = 0$, we see that there is a secondary minimum loss of 4.23% at $d_1/ka^2 = d_2/ka^2 = 0.0735$ due to favorable mixing of the HE_{11} and HE_{12} modes. There is a saddle point with loss 10.03% at $d_1/ka^2 = d_2/ka^2 = 0.0495$.

If one were to vary d_2 at constant d_1, one would observe a maximum output power at that value of d_2 at which $\partial \mathcal{L}/\partial d_2 = 0$, whereas if d_1 were varied at constant d_2, the power maximum would occur where $\partial \mathcal{L}/\partial d_1 = 0$. We have included a heavy solid line in Figure 3a to indicate where $\partial \mathcal{L}/\partial d_2 = 0$, and a heavy dashed line to indicate where $\partial \mathcal{L}/\partial d_1 = 0$. Note that although the loss contours are symmetric about the line $d_2 = d_1$, nevertheless the curves along which the partial derivatives are zero are not symmetric (although they are mirror images of one another.) The slope of the curve along which $\partial \mathcal{L}/\partial d_2 = 0$ is negative, consistent with the experimental observation that as d_1 increases, the value of d_2 at which power peaks decreases. The degree of quantitative agreement will be examined in the experimental section.

In Figure 3b we have presented a family of curves analogous to the heavy solid curve in Figure 3a, for a number of different values of the waveguide length parameter ℓ'/ka^2. These were all calculated using two waveguide modes, and with Re $\nu_n/ka = 0$. (For typical actual values of Re ν_n/ka, the curves will be shifted inward very slightly toward smaller values of d_1/ka^2 and d_2/ka^2.) We see that as ℓ'/ka^2 increases toward the value $4\pi/(u_{12}^2 - u_{11}^2) = 0.509$, for which the single-pass phase shift between HE_{11} and HE_{12} is 2π, the curves become more nearly straight lines and shift inward toward the origin. If ℓ'/ka^2 were slightly greater than 0.509, no loss minima would have been observed, and the losses would have increased monotonically as a

function of d_1 and d_2. As ℓ'/ka^2 was further increased, loss minima would reappear at large distances and move inward as ℓ'/ka^2 approached $8\pi/(u_{12}^2 - u_{11}^2)$. (If more waveguide modes were included in the calculation, other less pronounced minima would also be observed due to favorable mixing of the HE_{11} with the HE_{13} or other higher order waveguide modes, but the $HE_{11}-HE_{12}$ minima are the dominant ones, especially if waveguide losses are significant.)

Next, we looked at the effect of varying waveguide length while holding the mirror distances constant. The simplest case we considered was that of a symmetric cavity with mirror distances d, with losses calculated using only two waveguide modes. In Figure 4a we have plotted loss vs. ℓ'/ka^2 for four different values of d/ka^2. In all cases, Re $\nu_n/ka=0.002$. The curve for $d/ka^2=0$ is essentially a graph of the HE_{11} waveguide loss (plus a small truncation loss) vs. guide length. The curves for larger d/ka^2 display, in addition to the steadily increasing waveguide losses, coupling losses which are periodic in ℓ'/ka^2. The period is given by

$$\Delta\ell'/ka^2 = 4\pi/(u_{12}^2 - u_{11}^2)$$

and represents an increment of 2π in the $HE_{11}-HE_{12}$ phase shift in one pass through the waveguide.

When d/ka^2 is relatively small, as for example 0.02 in Figure 4a, the lowest loss mode is almost entirely HE_{11} except over a small range of values of ℓ'/ka^2 in which mixing with HE_{12} takes place, 0.45 to 0.50, 0.95 to 1.00, etc. for $d/ka^2=0.02$. Outside these mixing regions, the coupling losses are well described by the pure-HE_{11} theory of Abrams [2]. The mixing can either increase or decrease the coupling losses, and as ℓ'/ka^2 increases so as to enter a mixing region, the admixture of HE_{12} at first causes the losses to

decrease almost to the pure HE_{11} waveguide losses; then as the HE_{12} content increases further, the losses increase sharply to a value above the pure-HE_{11} coupling loss. The maximum is not reached until the HE_{12} content has already begun to decrease again; then as HE_{12} content decays to zero, the coupling loss again approaches that for pure HE_{11}.

As d/ka^2 increases, the mixing regions broaden and shift toward smaller ℓ'/ka^2, and the amplitude of the loss variation due to mixing increases, but the loss minimum does not come as close to the pure HE_{11} waveguide loss. This is illustrated by the curves for $d/ka^2 = 0.04$ and 0.06 in Figure 4a.

For very small values of the waveguide loss parameter Re ν_n/ka, the minimum loss occurs when about 14% of the power is in the HE_{12} mode. This appears to be true for a wide variety of values of d/ka^2. In this case, the minimum loss is produced strictly by minimizing the coupling losses. Note that there is also a high-loss cavity configuration at slightly larger ℓ'/ka^2 for which the HE_{12} content is also 14%. This illustrates that the relative phases of the modes, and not just their amplitudes, are important. For larger values of Re ν_n/ka, there is a tradeoff between coupling losses and waveguide losses, and the loss minimum occurs for a smaller HE_{12} mode content.

While still restricting our calculation to the use of two waveguide modes, we explored the effects of cavity asymmetry on the length dependence. In Figure 4b we present graphs of loss vs. ℓ'/ka^2 for three different cavities of varying asymmetry, starting from a completely symmetric cavity ($d_1 = d_2$) and progressing to a maximally asymmetric cavity ($d_1 = 0$, d_2 large). The values of d_1/ka^2 and d_2/ka^2 were chosen to lie on a curve like the ones in Figure 3b, so that the loss minima would continue to occur at roughly the same values of ℓ'/ka^2. The value of Re ν_n/ka was again 0.002.

We see that introducing asymmetry produces new regions of mode mixing, resulting in new minima and maxima appearing midway between those obtained with the completely symmetric cavity. As the cavity becomes more asymmetric, these new minima and maxima become more pronounced, until for the maximally asymmetric cavity they become equally as strong as the original set of minima and maxima observed for the symmetric cavity. The coupling losses are then periodic in ℓ'/ka^2 with a period of half that for the aymmetric cavity. This can be understood easily by noting that as d_1 goes to zero, the cavity becomes equivalent to the half-cavity of a symmetric resonator having waveguide length 2ℓ and both mirror distances equal to d_2. The periodicity of the coupling losses for the latter resonator is then

$$\Delta(2\ell'/ka^2) = 4\pi/(u_{12}^2 - u_{11}^2)$$

so that $\Delta\ell'/ka^2$ is half what it was for the symmetric resonator.

Next, returning to the symmetric cavity, we examined the effect of varying the number of waveguide modes used in the calculation. In Figure 5a we plot loss for the lowest loss-mode calculated for $d/ka^2=0.04$ and $Re\ v_n/ka=0.002$ using one, two, and three waveguide modes. The curve for two modes was the same that appeared in Figure 4a for $d/ka^2=0.04$. The curve for just one waveguide mode is nearly a straight line (saturating at much larger ℓ'/ka^2) whose intercept at $\ell'/ka^2=0$ is just the pure-HE_{11} coupling loss that would be calculated from the theory of Abrams [2], and whose slope is the same as that of the waveguide loss curve (the curve for $d/ka^2=0$ in Figure 4a.)

Going from two modes to three modes clearly produces a non-negligible effect. There are now a new series of loss minima due to mixing of the HE_{11} and HE_{13} modes, having spacing

$$\Delta \ell'/ka^2 = 4\pi/(u_{13}{}^2 - u_{11}{}^2)$$

There are also new loss maxima and, in a few places, sharp cusps, the nature of which will become apparent when we examine Figure 5b. We could expect further such complications from using four or more waveguide modes. However, for larger values of Re ν_n/ka, the effect of adding a third mode becomes less significant except at very small values of ℓ'/ka^2. Also, there is very little change in the loss curve in the vicinity of the loss minimum due to HE_{11}-HE_{12} mode mixing. Finally, as one goes to larger values of d/ka^2, the effect of the third mode becomes less pronounced on the whole, although the broadening of the region in which HE_{11}-HE_{13} mixing occurs results in a slightly greater perturbation in the vicinity of the HE_{11}-HE_{12} minimum, and a small shift in the position of the minimum.

When we use three waveguide modes, the matrix we are diagonalizing is 3×3, and we obtain three loss solutions. Thus far we have been looking at only the lowest-loss solution, but in Figure 5b we plot the losses of all three resonator modes. A number of interesting features are revealed. First, the sharp cusp in the losses for the lowest-loss mode at $\ell'/ka^2=0.445$ is actually a crossover between two solutions, i.e., a point of mode degeneracy. Such degeneracies can also occur when the calculation is done using only two waveguide modes, but only for very small values of Re ν_n/ka. In our three-mode calculation, conditions of mode mixing similar to those at $\ell'/ka^2=0.445$ also occur at $\ell'/ka^2=0.96$, but due to the higher waveguide losses, the mode mixing is no longer strong enough to produce degeneracy.

At those values of ℓ'/ka^2 where the lowest-loss mode has loss minima, the losses are very high for the next-lowest-loss resonator mode. On the

other hand, there are values of ℓ'/ka^2 where the modes are degenerate or nearly degenerate, and at such places we can expect poor stability of the mode pattern. We have already mentioned the degeneracy that occurs at $\ell'/ka^2 = 0.445$ between two resonator modes, each of which is made up primarily of HE_{11} and HE_{12} waveguide modes. Another sort of degeneracy occurs at $\ell'/ka^2 = 0.20$. The second-lowest-loss mode has a series of minima occurring at $\ell'/ka^2 = 0.20$, 0.48, 0.76, 1.04, etc., due to favorable mixing between the HE_{12} and HE_{13} modes. These minima have a spacing

$$\Delta \ell'/ka^2 = 4\pi/(u_{13}{}^2 - u_{12}{}^2)$$

The first of these minima is approximately degenerate with the lowest-loss, predominantly-HE_{11} mode, since the lowering of coupling losses due to interference between the diffracted HE_{12} and HE_{13} modes compensates for their higher waveguide losses. For smaller values of d/ka^2 and/or Re v_n/ka, the losses for this HE_{12}-HE_{13} mixture can actually drop below those of the mostly-HE_{11} resonator mode.

An overview of the dependence of coupling losses on both waveguide length ℓ'/ka^2 and mirror distance d/ka^2 for a symmetric cavity is provided by the loss contour plot in Figure 6, calculated for Re $v_n/ka = 0.002$. This plot was calculated using only two waveguide modes, and is not intended to be quantitatively accurate in most regions, but it exhibits qualitatively some important features. The loss contour for some particular low loss value (such as the 5% loss contour) stays close to the vertical axis for most ℓ'/ka^2. However, in the vicinity of a particular diagonal line $(\ell'+2d)/ka^2$ =const., the contours extend out to much larger values of d/ka^2. There is a valley in the contour plot along this line. Slightly above this, the con-

tours are drawn in toward smaller values of d/ka^2; this corresponds to a ridge in the contour plot, and to the peaks in the graphs of loss vs. ℓ'/ka^2 in Figure 4a. Since the coupling losses are periodic in ℓ'/ka^2, there will be other such valleys and ridges occuring at higher values of ℓ'/ka^2.

We have drawn in two heavy curves on the contour plot. The solid heavy curve is the curve along which $\partial\mathcal{L}/\partial\ell'=0$, and represents the optimum choice of waveguide length for a given mirror distance. The dashed heavy curve is the curve along which $\partial\mathcal{L}/\partial d=0$, and represents an optimum choice of mirror distance for a given waveguide length. (That is, if one cannot place the mirror close to $d=0$, then a value of d/ka^2 along this curve is the best choice to minimize cavity losses.) The dashed curve terminates at $\ell'/ka^2 =0.11$ because below this value, the losses increase monotonically with d/ka^2, and there is no d for which $\partial\mathcal{L}/\partial d=0$. A similar interval with no optimum d occurs between $\ell'/ka^2=0.51$ and 0.62, as was discussed earlier in the context of loss contours in the d_2/ka^2 vs. d_1/ka^2 plane, an interval of waveguide phase shifts slightly greater than 2π but much less than 4π.

The valley and ridge in the contour plot in Figure 6 are due to mixing between the HE_{11} and HE_{12} modes. If further modes are used in the calculation, additional valleys and ridges will appear. For small d/ka^2, the valleys due to mixing between the HE_{1m} and HE_{11} modes will fall roughly along the straight lines

$$(\ell' + 2d)/ka^2 = 4\pi N/(u_{1m}^{\ 2}-u_{11}^{\ 2}) \tag{7}$$

where N is a positive integer. These become increasingly closely spaced as m increases, but the larger m is the less significant the influence of the HE_{1m} mode on the loss contours at large d/ka^2, and also at large ℓ'/ka^2 if Re ν_n/ka is large.

Since the optimal choice of ℓ'/ka^2 for a given d/ka^2 or vice versa is such that $(\ell'+2d)/ka^2$ is nearly a constant over a rather wide range of values of the independent variable, more precise information can be conveyed by plotting an optimum effective total cavity length L'/ka^2, where

$$L' \equiv \ell' + 2d \qquad (8)$$

as a function of d/ka^2 or ℓ'/ka^2. In Figure 7a we present a family of curves of L'/ka^2 vs. d/ka^2 such that $\partial \mathcal{L}/\partial \ell'=0$, corresponding to the solid curve in Figure 6, but for a variety of different values of Re ν_n/ka, and caclulated using three rather than two waveguide modes. If one were trying to design a waveguide laser resonator with a waveguide radius a and a minimum practical mirror distance d, then one would use this graph to select an optimum value of the total effective cavity length L', from which one could find the optimum ℓ' by subtracting 2d, and determine the actual waveguide length ℓ if Im ν_n were known. (If not, it usually adequate to assume that Im $\nu_n=0$ and $\ell=\ell'$.) Given that one chooses ℓ' in this way, the overall resonator loss that can be achieved for various values of Re ν_n/ka is plotted vs. d/ka^2 in Figure 7b. For comparison, we have also plotted the coupling losses from the pure-HE_{11} model [2] with no waveguide losses included. It is apparent that the interference between the HE_{11} and HE_{12} modes allows vastly lower losses to be achieved out to much larger values of d/ka^2 than one would have expected from the pure-HE_{11} model. The losses do not begin increasing rapidly above the waveguide losses until $d/ka^2 \approx 0.10$.

One feature of the curves in Figures 7a and 7b that requires explanation is the following: Some of the curves terminate at small values of d/ka^2, and the larger the value of Re ν_n/ka, the larger the value of d/ka^2

at which they terminate. This is because at small d/ka^2, the waveguide losses dominate over the coupling losses. As one passes through a region of mode mixing along a line of constant d/ka^2, the resonator losses are at first reduced below, and then increased above, the monotonically increasing curve representing waveguide plus pure-HE_{11} coupling losses vs. ℓ'/ka^2 (Figure 4a). If the increase in waveguide loss with ℓ'/ka^2 is rapid enough, the small change in losses due to mode mixing is not enough to ever make the slope of the loss curve change sign. Thus there is no value of ℓ'/ka^2 such that $\partial\mathcal{L}/\partial\ell'=0$ for small values of d/ka^2.

Another situation encountered in designing a resonator is selection of the mirror distances, given a waveguide of length ℓ and radius a. In Figure 8a we plot curves of L'/ka^2 vs. ℓ'/ka^2 along which $\partial\mathcal{L}/\partial d=0$, again calculated for a symmetric cavity for various values of Re ν_n/ka using three waveguide modes. The information here is analogous to that in the dashed curve in Figure 6. Given the actual waveguide length ℓ, one would calculate ℓ' from Equation (6) and use Figure 8a to determine the total cavity length L', then find the mirror distance from Equation (8).

The cavity losses obtained by selecting the mirror distances according to the above procedure are plotted in Figure 8b. Cavity losses remain small, dominated by the waveguide losses, over the range $0.30<\ell'/ka^2<0.509$, and over that same range the optimum total cavity length L'/ka^2 remains nearly constant. The curves terminate at $\ell'/ka^2\approx0.06$, somewhat below the value at which the dashed curve in Figure 6 terminated; this extension is due to the effect of including the HE_{13} mode in the calculations. The curves for different Re ν_n/ka all converge as ℓ'/ka^2 becomes small, since for short waveguides the waveguide losses become small, and the task of minimizing the

total cavity losses becomes essentially identical to minimizing the coupling losses.

Often one of the dominant considerations in the design of a waveguide laser is the free spectral range $\Delta\nu=c/2L$ of the resonator, where $L=\ell+2d$ is the total cavity length. Let us assume for simplicity that $\ell'=\ell$ and hence $L'=L$. If we specify $\Delta\nu$, this determines L, and Figures 7 and 8, together with the known periodicity of the $HE_{11}-HE_{12}$ mode mixing effects, tell us we want $L/ka^2 \simeq 0.5N$, where $N=1,2,3,\ldots$. For a laser that is to operate at wavelength $\lambda=2\pi/k$, we therefore want the waveguide bore radius to be

$$a \simeq (c\lambda/2\pi N\Delta\nu)^{\frac{1}{2}} \qquad (9)$$

For example, at $\lambda=10.6\mu m$, if we want $\Delta\nu=500$ MHz, this gives L=30 cm and $a\simeq 1$ mm, or about a 2 mm bore; for $\Delta\nu=1$ GHz, we obtain L=15 cm and $a\simeq 0.71$ mm, or about a 1.4 mm bore, in both cases assuming N=1. These are both quite reasonable dimensions for CO_2 waveguide lasers. The only case in which one would consider $N\neq 1$ is when the value of a obtained for N=1 is too large, so that the gain and saturation parameter are too low and/or the pressure broadening at obtainable operating pressures for that bore radius is insufficient to allow tuning over the entire free spectral range.

Having thus estimated a desirable tube diameter, one is then faced with a number of tasks such as finding the closest bore diameter available commercially; determining the changes in the design necessitated by the difference between that and the desired diameter; making certain that variation of the bore diameter within the manufacturer's tolerance will not result in high losses; obtaining the best compromise in the design to operate over the entire range of desired wavelengths; using Im ν_n, if known, to refine the

design by relaxing the assumption that $\ell'=\ell$; and determining whether an external-mirror construction is feasible. If the total cavity length is constrained to be constant, with $L/ka^2 = 0.5$, then the losses increase monotonically with d so that it is desirable to make d as small as possible. Both from the standpoint of keeping losses small and of satisfying the approximation that the optimum total cavity length is constant, independent of d/ka^2 or ℓ'/ka^2, it is necessary that $d/ka^2 < 0.10$, and conversely, $\ell'/ka^2 > 0.30$. In the preceeding examples, for the 2 mm bore laser with $\Delta v = 500$ MHz, this means d<6 cm, which is easily achieved in an external-mirror laser. But for the 1.4 mm diameter laser with $\Delta v = 1$ GHz, we require d<3 cm, which might be more easily achieved in an internal-mirror design.

Thus far we have seen that a certain narrow range of values of L'/ka^2 is preferred in order to keep cavity losses low. Changing the wavelength $\lambda = 2\pi/k$ will shift the range of preferred L' values. This has two consequences for lasers exhibiting gain over a range of wavelengths.

First, in a cavity with no wavelength-selective element, the cavity length itself can exert a sort of coarse wavelength selectivity. For a laser with a particular waveguide length and bore diameter, with one of the mirror distances, d_1, held constant, the losses for several different laser wavelengths (for example, the various bands and branches of CO_2 laser transitions in the 9-11 μm range) will have minima at different values of the mirror distance d_2, and when the loss is minimized for one wavelength, the losses for the other wavelengths may be much higher. The farther away the other wavelengths are, the better they are discriminated against; also, since shorter wavelengths have loss minima at larger values of d_2, and since losses increase more rapidly on the large-d_2 side of the minimum than on the small-d_2

side, discrimination is better against longer wavelengths than against shorter wavelengths. The selectivity is enhanced by the existence of competition between laser transitions. This sort of selectivity is too coarse to allow selection of one particular CO_2 laser line, but can select which branch of which band the laser operates on, beyond which it may be possible to select a few individual laser lines within each branch by piezoelectrically tuning the longitudinal mode frequencies [13], provided that the pressure broadening is not too large. For a laser of ~ 2.38 mm bore such as ours, about 6 cm of mirror translation is expected to be required to tune the laser from the 10 μm P-branch to the 9 μm R-branch; for smaller-bore lasers, smaller changes in length are needed.

The second consequence pertains to grating-tuned lasers. The optimum position of one mirror shifts as we tune the wavelength while holding the other mirror position fixed. If the wavelength is tuned without simultaneous adjustment of the cavity length, the losses will be high over part of the tuning range, and the range may be restricted. This suggests that in grating-tuned waveguide lasers, the grating should be mounted on a translation stage that is slaved to the grating rotation control, so that as the grating is tuned toward longer wavelengths, it also translates toward the laser tube. While for large-bore lasers such as ours, many centimeters of translation are needed, the change in cavity length needed for a given change in wavelength is proportional to the square of the bore radius, so that, for example, only a 2.5 cm change in cavity length is needed to cover the 9.2-10.8 μm range with a 1.4 mm bore laser.

To complete the theory section, we discuss our physical interpretation of the origin of the loss minima. As discussed earlier, for $w_o/a \simeq 0.55$,

there is a strong coupling both between the HE_{11} and TEM_{00} and between the HE_{12} and TEM_{10} modes. To a rough approximation, the field in the waveguide can be considered a superposition of just the HE_{11} and HE_{12} modes, while the field in the free space region can be considered a superposition of just TEM_{00} and TEM_{10}. Individually, each of these two free space modes diverges as it propagates from the waveguide aperture to the mirror and back. However, if their initial relative amplitudes and phases and the relative phase shifts they undergo in propagating to the mirror and back are right, the two returning TEM modes will interfere constructively near the center of the beam, but destructively, so as to produce nearly complete cancellation, in the outer edges. This superposition therefore has its power concentrated within a much smaller radius than either the returning TEM_{00} or TEM_{10} modes individually, and a large fraction of the power can be coupled back into the waveguide. The returning beam then couples to a different superposition of HE_{11} and HE_{12}, which must undergo the right relative phase shift and attenuation or gain in the waveguide to produce a similar low loss at the other end. In the limit as the mirror distances go to zero, the optimum waveguide length approaches that for which the single-pass relative phase shift between HE_{11} and HE_{12} is $2\pi N$ (where N=1,2,3,...); for small finite mirror distances, the minimum loss condition is roughly that the HE_{11}-HE_{12} phase shift in the waveguide plus the TEM_{00}-TEM_{10} phase shifts in the free space regions add up to $2\pi N$.

III. Experiment

The laser used for this experiment has been described previously elsewhere [5]. Briefly, it consists of an alumina tube resting in a groove in a water-cooled aluminum block. Stainless steel swage tees are attached to the

ends of the ceramic tube using teflon ferrules, and serve both as electrodes and as conduits for the flowing gas. The ends of the tees are milled off at Brewster's angle, and NaCl windows are attached directly. This design is uniquely suited for our experiment, since the length of the waveguide can be varied easily without extensive rebuilding of the laser.

Due to the structure of our laser, the minimum distances d_1 and d_2 for which we could make measurements were 4 cm. The minimum ℓ was 28 cm, limited by the length of the heat sink. The tubes used as waveguides were from McDanel Refractory Porcelain Co., and were made of extruded type AP-35 alumina, which is 99% pure Al_2O_3. Nominal inner diameters for the tubes were (2.38±0.08)mm. Since variations in tube diameter within this tolerance were sufficient to affect predictions considerably, and since variations nearly as large as the manufacturer's tolerance were in fact observed, we found it necessary to measure our tube diameters using a microscope with a precision positioning platform and digital readout. This permitted determination of the bore diameter to within an accuracy of ±0.002 mm.

A few measurements were made with another laser similar to that described above, but with a nominal bore diameter of (1.59±0.08)mm and an 11.5 cm guide length. The waveguide material was again extruded alumina.

We did not measure the cavity losses directly, but instead observed the variation of the laser output power, which is a monotonically decreasing function of the cavity losses, with changes in the cavity configuration. Configurations giving a maximum power corresponded to loss minima and vice versa. Thus, what we compared to theory was not the actual value of cavity loss, but the cavity configurations for which the derivative of loss with respect to some cavity dimension was zero.

The mirror distances were measured to an accuracy of ±0.1 cm, more than adequate for our purposes. To the measured distances were added a correction

$$\delta d = t \ (n^2 - 1)/(n^2 + 1)^{\frac{1}{2}} \tag{10}$$

where t is the thickness and n the refractive index of the Brewster window. This represents the difference between the measured geometrical distance and the effective optical distance from the waveguide to the mirror. For a sodium chloride window of thickness t=4 mm and refractive index n=1.4948, this correction is 2.7 mm. Once power was measured as a function of mirror distance, the location of the peak could be estimated to within typically about ±0.25 cm.

Our first observation, mentioned at the beginning of the paper, was of output power versus one mirror distance, d_2, for various fixed values of the other mirror distance, d_1, for a waveguide of length 28 cm and bore diameter 2.435 mm. These data were presented in Figure 2. We also obtained some similar data with the smaller laser of length 11.5 cm and bore diameter 1.666 mm. From the curves in Figure 2 and those for the smaller laser, we determined minimum-loss d_2 values for each d_1, and plotted them in Figure 9, along with theoretical curves for the two respective waveguides. The theoretical curves were calculated using three waveguide modes, and unlike the two-mode curves in Figure 3, they display discontinuities. The loss itself is a continuous function of d_1 and d_2, but the loss vs. d_2 curve at fixed d_1 has a broad, flat-bottomed valley, and at a certain value of d_1, the position of the minimum shifts from one side of the valley to the other, resulting in a jump in the optimum d_2 vs. d_1 curve. The experimental points fall some-

what above the theoretical curves, a fact on which we will comment later. We note that the highest power obtained with a flat-mirror resonator, 4.79 W, is not much smaller than the 5.88 W we obtained under the same conditions of pressure and current for a resonator consisting of 34 cm radius of curvature placed at their optimum distance of 34 cm from the ends of the waveguide. This difference in power is entirely attributable to the difference in output coupling for the two output mirrors: 5% for the flat mirror and 7% for the curved mirror. Thus the benefits of going to a curved-mirror resonator are not very great, and may be outweighed by the fact that the curved-mirror resonator requires a greater total cavity length in order to achieve maximum output. Further improvement in the flat-mirror laser could be achieved by lengthening the waveguide so that the optimum mirror distances were approximately equal to the minimum mechanically accessible distances of 4 cm.

Next, we measured output power as a function of mirror distance d and waveguide length ℓ for symmetric cavities with $d_1 = d_2 \equiv d$. We did measurements for 36 different values of ℓ ranging from 28 cm to 45.7 cm. The same tube, having a measured bore diameter of 2.376 mm, was used throughout, and segments of approximately 0.5 cm were cut off with a diamond saw for each new length. After cutting, the tube was cleaned with water and dried. The water-cooled heat sink block used was 22.6 cm long, not sufficient to cool the entire length of the waveguide except for the shortest lengths used. For longer waveguide lengths we cooled the remainder of the tube with Eimac type HR-8 finned aluminum heat sinks which we drilled out to accomodate the tube outer diameter, and which we air-cooled with fans.

For all measurements we maintained the same average pressure of 42 Torr, and a pressure gradient of roughly 0.07 Torr/cm, in the waveguide. The

pressure was well below optimal, but was the maximum for which our power supply could maintain a discharge for the longest tube lengths used. The current was 10 mA throughout.

Considerable scatter in the data was caused by variations in the straightness of the tube. Large variations in output power, by as much as 65%, could be produced by varying the rotational orientation of the waveguide within its groove or by applying pressure to one side of the tube to cause it to bend in a particular direction. Our later measurements were made with pressure applied to the tube in such a way as to maximize the power, but for our earlier measurements (i.e. for longer tube lengths) this was not done, and there is more scatter in the data. Also, contamination of the Brewster windows by the grease used on the heat sinks sometimes resulted in window damage and consequent anomalous power measurements.

For each value of the waveguide length ℓ, we observed the variation of output power with the mirror distance d. Within each of these runs, factors such as bore straightness and condition of the windows tended to be constant, and relatively clean-looking data were obtained. While, for example, rotating the tube in the groove could produce a considerable variation in the maximum power obtainable, it had much less effect on the value of d at which maximum power was observed. Examples of experimental data on power vs. d at constant ℓ, and on power vs. ℓ at constant d, appear as inserts in Figure 10. Due to the problems noted in the preceding paragraph, there is much more scatter in the power-vs.-ℓ data, expecially since each such graph contains data obtained over a period of about a month.

In the plots of power vs. d at constant ℓ for the longer waveguide lengths ($\ell \geq 36$ cm) the peak in power due to HE_{11}-HE_{12} mode mixing occurs at

d<4 cm, which is inaccessible to us. For $\ell \leq 35.5$ cm the peak does occur at
d>4 cm, and moves outward toward larger d as ℓ decreases, as expected. The
graphs for $\ell=44$ through 45.7 cm exhibit a lesser peak which we attribute to
the $HE_{11}-HE_{13}$ mode mixing loss minimum. These peaks occur at total cavity
lengths of about 59 to 59.5 cm, as compared to 60.9 cm predicted theoreti-
cally for the fourth $HE_{11}-HE_{13}$ minimum. Where these peaks were observed the
laser output was observed to be a donut mode. This is easily understood
since the HE_{11} mode couples strongly to a TEM_{00} free space mode, while the
HE_{13} couples strongly to a TEM_{20} mode. In order for the TEM_{20} and TEM_{00}
modes to produce destructive interference in the outermost edges of the beam,
and thus reduce coupling losses by reducing the effective spot size, they
must also interfere destructively at the center of the beam while reinfor-
cing each other at intermediate radii. This results in a donut mode pattern.
The laser mode pattern observed for the $HE_{11}-HE_{12}$ loss minimum was always
clean and Gaussian-looking, although we did not do any quantitative measure-
ments of beam profile.

The theoretical graphs of loss vs. ℓ in Figures 4 and 5 lead us to ex-
pect a maximum in loss, and hence a minimum in power, at values of ℓ slight-
ly longer than those for which a peak power is observed due to $HE_{11}-HE_{12}$
mixing. These power minima are very indistinct, if in fact present at all,
in the power vs. ℓ plots such as the insert in Figure 10. It is likely that
the minima are being washed out by the tendency of the laser to switch to a
shorter wavelength transition, for which the losses are smaller, rather than
continue to operate at 10.6 µm. We will return to the wavelength shift ques-
tion shortly. We also expect additional loss minima/power maxima at still
larger values of ℓ, due to $HE_{11}-HE_{13}$ mixing. The third such loss minimum

is generally very close to the HE_{11}-HE_{12} minimum (see Figure 5), and that together with the ability of the laser to switch wavelengths to avoid higher losses at intermediate ℓ values results in this loss minimum, and the consequent peak in power, being unresolved from the HE_{11}-HE_{12} peak. The fourth HE_{11}-HE_{12} loss minimum is expected to occur at such long total cavity lengths that for the largest d value shown, it should occur near the largest ℓ used, and for smaller d it should not be seen. However, for large d the loss minimum is not expected to be very strong. The data show no distinct peak in power distinguishable from the noise.

From plots such as those in the inserts in Figure 10 (mainly the power-vs.-d graphs) we obtained a number of points on an optimum d vs. ℓ curve; these are compared to theory in Figure 10. The data lie approximately on a straight line of constant total cavity length, as expected from theory, but that length is somewhat longer than predicted.

In a cavity with no wavelength-selective element we predicted that as the total cavity length was extended beyond the optimum value for 10.6 µm, so that losses became very high at that wavelength, the laser would switch to shorter-wavelength transitions, for which the losses are lower. Figure 11a shows an example of this phenomenon. Output power is plotted as a function of mirror distance d_2 at constant d_1=10.3 cm for a laser with waveguide length ℓ=30.5 cm and bore diameter 2a=2.428 mm. Also indicated are the bands and branches for which lasing was observed for various ranges of d_2 values. For small values of d_2 the laser operated in the 10 µm P-branch; as d_2 was increased, it switched to 10R, then 9P, and finally 9R. There was some overlap in the intervals in which certain branches could be obtained, but for each branch there was some range of d_2 in which only that branch would lase.

This illustrates the coarse wavelength selectivity that can be achieved by varying the total cavity length. The appearance of different branches and bands is also marked by shoulders on the power-vs.-d_2 curve.

We find that the range of d_2 over which each branch lases is farther from the waveguide than we would have expected from our theory. Also, our theoretical loss curves (not shown) suggest that the hardest branch to select by this method should be 10R, whereas in fact we found it generally most difficult to obtain 9P, and for most of the cavity configurations we examined other than this one, the laser skipped over this branch.

The other consequence of wavelength variation we predicted was that as a grating-tuned laser was tuned toward shorter wavelengths, the cavity would have to be lengthened in order to maintain low losses. An example of this is provided in Figure 11b. This time we have ℓ=28 cm and 2a=2.435 mm, and the grating was held at constant distance d_1=7.3 cm while the distance d_2 to the other flat mirror was varied. Power is plotted vs. d_2 for the strongest line in each branch. The expected shift is observed, about a 5 cm lengthening in the optimum cavity length in going from 10.588 to 9.268 μm.

IV. Discussion

Our experimental results are generally in good qualitative agreement with our calculations, but insofar as quantitative comparison is possible (mainly in the positions of loss minima) there are slight discrepancies, particularly that the loss minima due to HE_{11}-HE_{12} mixing occur at greater total cavity lengths than predicted. Among the explanations that might be proposed are:

1) Inaccuracy or nonuniformity of the waveguide bore radius;

2) Use of an incorrect value of the material parameter ν_n;

3) Effects due to waveguide modes of higher order than HE_{13};

4) Effects due to wavefront curvature of the individual HE_{1m} modes [14]; and

5) Effects due to the active gain medium.

A single measurement of the tube diameter was accurate to ±0.002 mm, or ±0.1% for a 2.38 mm bore, far too small an uncertainty to account for the observed discrepancy. A more serious question concerns the uniformity of the bore diameter of the extruded tube. In only one case have we measured diameters of more than one segment of the same tube, that being the tube that was progressively shortened from 45.7 cm to 28 cm. We found the variation in bore diameters for those pieces to be less than 0.5%, still too small to be responsible. In fact, even the manufacturer's tolerance in the tube diameter is not quite sufficient to explain the discrepancy. While we cannot rule out variations of the bore diameter in places we did not measure, we think it unlikely that this is the cause of the disagreement.

The complex material parameter ν_n defined in Equation (4) is a function of the complex refractive index ν of the waveguide material. To our knowledge, no refractive index measurements on alumina ceramic have been reported, although there have been measurements for ruby [15] and sapphire [16], crystalline materials of nearly the same composition. While we are not completely convinced of the applicability of these data to alumina, Abrams and Bridges [17] have used the data for ruby to estimate Re ν_n for alumina. Using the same refractive index data [15], we were unable to reproduce their Re ν_n values for alumina below about 1000 cm^{-1}. We therefore present in Table I the values of Re ν_n and Im ν_n that we calculated for the most prominent CO_2 laser transition wavelengths. Since ruby is birefringent, one obtains different values of ν_n for electric fields parallel and perpendicular

to the c-axis of the crystal. Alumina is a fine-grained polycrystalling material, so we assumed, as did Hall et al. [18], that ν_n could be found by averaging over the random crystal orientations. This procedure was used in obtaining the values of ν_n listed in Table I. Values of ν_n for 10P(20) in this table were used in finding the theoretical curves in Figures 9 and 10.

The relation between effective and actual waveguide lengths, ℓ' and ℓ, respectively, was given in Equation (6). For a CO_2 waveguide laser with a=1.19 mm, ka$\sim$700, so that Im ν_n would have to be more than an order of magnitude larger than the value we used in order to bring theory into agreement with experiment. While we are uncertain of the accuracy of the ν_n values in Table I, we think it unlikely that they are an order of magnitude too low. Deviations of Re ν_n may, however, explain the fact that the 9 μm P-branch was hard to obtain by varying the cavity length; perhaps Re ν_n is larger there than we have supposed, so that the waveguide is particularly lossy.

Both of the above proposed explanations assumed that ℓ'/ka^2 was not what it seemed, either because a was not accurately known, or because the wrong value of Im ν_n was used in converting from ℓ to ℓ'. In either case, all other loss minima due to waveguide mode mixing should be affected in a consistent manner. This is not the case, however. Whereas experimentally the $HE_{11}-HE_{12}$ loss minima occur at cavity lengths longer than predicted, the $HE_{11}-HE_{13}$ minima occur at lengths slightly smaller than predicted.

We limited our calculations to use of a maximum of three waveguide modes, and it is possible that higher order modes may be important in determining the position of the loss minimum. Abrams and Chester [8] used at least 5 modes in all their calculations, but found that increasing the num-

ber from five to ten made little difference. Degnan and Hall [3] found that three modes were adequate to account for most observed features of their experimental data. We have found that going from two to three modes can make large changes in the losses at small d/ka^2 (see Figure 5), but has little influence on the positions of loss minima since the regions of mode mixing are relatively narrow and do not overlap. At larger d/ka^2, however, the mixing regions are broader and overlap substantially, and while the change in losses in going from two to three modes is much smaller than at small d/ka^2, there can be a significant shift in the position of a minimum. For our laser with a 2.38 mm bore, the predicted optimum cavity length increases by >1 cm in going from two to three modes whenever d>8 cm. For a higher mode to have as large an effect, not only the strength of that mode's mixing with HE_{11} is important, but also the overlap of the mixing region with that region in which strong HE_{11}-HE_{12} mixing occurs. Based on what we have learned about the locus of HE_{1m}-HE_{11} mixing on the ℓ/ka^2 vs. d/ka^2 plot, we estimate that both HE_{14} and HE_{15} mixing are likely to be present in the neighborhood of the HE_{11}-HE_{12} loss minimum, but we cannot predict whether it will be strong enough to shift the minimum very much.

Tacke [14] has shown that any waveguide losses in excess of those due to the leaky nature of the waveguide [6], such as due to scattering from surface imperfections, will induce a curvature of the wavefronts of the individual HE_{1m} modes, in excess of the curvature of order λ/a calculated by Marcatili and Schmeltzer [6] for those modes, and distinct from the overall wavefront curvature that is present because the actual field is a superposition of HE_{11}, HE_{12}, and higher order waveguide modes. This curvature of the HE_{1m} wavefronts will alter the coupling to the free space TEM modes.

It is known from the experiments of Hall et al.[18] that real waveguides, and especially extruded ones, have guiding losses well in excess of those calculated for the idealized leaky waveguide [6], so perhaps this effect contributes to the discrepancies. At this point we cannot quantitatively evaluate the effect because it would require a knowledge of the actual waveguide attenuation factors for all modes that are important (whereas only that for HE_{11} can be measured conveniently) and because the theory has not been worked out completely for higher order modes.

Finally, we have neglected the active gain medium in the laser. This medium will generally have a nonuniform radial gain dependence and will produce a mixing of the waveguide modes as well as different gains for the different modes. Thus matrix M_5 will be non-diagonal, and the relative magnitudes of its diagonal elements will be different. Considering only the second effect, we have done rough calculations that indicate that if the HE_{12} mode has a higher gain than the HE_{11}, this will shift the optimum ℓ vs. d curve in the direction of the experimental data. While the active gain medium may be of some importance, we doubt that it is the most important correction, because in experiments in which we varied the laser pressure and current, and hence the characteristics of the active gain medium, the optimum cavity configurations did not change significantly, if at all.

It appears possible that some combination of these last three effects (higher waveguide modes, wavefront curvature due to excess losses, active gain medium) may be responsible for the observed disagreement between theory and experiment, but we are not presently able to evaluate them quantitatively.

V. Conclusions

We have presented a new approach to the calculation of waveguide laser

resonator losses for the specific case of a circular dielectric waveguide and flat mirrors. This method has the advantage of minimizing the amount of numerical integration and therefore greatly reduces computation time.

Our calculations using this method predict that low losses can be achieved for a flat-mirror resonator even for rather large waveguide-mirror distances, provided that a certain relationship between the waveguide length and mirror distance is satisfied. For $d/ka^2 < 0.10$, that relation is simply that the total cavity length should equal a constant depending on the wavelength and the waveguide bore radius; when this is satisfied, overall resonator losses only slightly exceed the waveguiding losses. Experimentally determined optimal cavity configurations are nearly in agreement with these predictions, but occur at somewhat greater total cavity lengths. The possibility of achieving low losses with a flat-mirror resonator has the important consequence of allowing the laser to be operated without specially-made short-radius concave mirrors.

In addition, it has been predicted and experimentally demonstrated that in a cavity without any wavelength-selective element, coarse wavelength tuning can be achieved simply by variation of the cavity length over several centimeters, and that conversely, in a grating-tuned laser, the cavity length must be changed as the wavelength is tuned in order to remain in a low-loss configuration.

Possible extensions of our method include the calculation of far-field radiation patterns and the generalization of the method to curved-mirror cavities. Also, a variant of our method could be used to treat the problem of the transmission of a Gaussian beam through a waveguide [19].

A computer program in the BASIC language for computation of resonator

losses is available from the authors [20], and a FORTRAN version is planned.

Acknowledgments

Appendix

We present here the details of the calculations of matrices M_1 through M_7.

In evaluating the matrix elements of M_1, we require normalized functions for both the waveguide and free space modes. These are given by, respectively,

$$HE_{1m}: \quad \phi_m(r) = \begin{cases} \dfrac{1}{\sqrt{\pi} \, |J_1(u_{1m})| \, a} \, J_0(u_{1m} \, r/a) & (r \leq a) \\ \\ 0 & (r > a) \end{cases} \qquad (A1)$$

$$TEM_{m0}: \quad \psi_m(r) = \sqrt{\frac{2}{\pi}} \, \frac{1}{w_o} \, L_m(2r^2/w_o{}^2) \, \exp(-r^2/w_o{}^2) \qquad (A2)$$

where J_0 and J_1 are Bessel functions, L_m is a Laguerre polynomial, and u_{1m} is the m'th zero of $J_0(u)$. The Laguerre polynomials are defined as in Magnus et al. [21], differing by a factor of $1/m!$ from the definition appearing in some other references. The matrix elements of M_1 are then given by

$$(M_1)_{mn} = 2\pi \int_0^a r \, \psi_m(r) \, \phi_n(r) \, dr \qquad (A3)$$

We calculate these elements by numerical integration using Simpson's rule with 101 mesh points. We then obtain matrix M_4 by taking the transpose of M_1.

The elements of the diagonal matrix M_2 are complex exponentials representing the phase shifts of the TEM_{m0} modes relative to the TEM_{00} mode in propagating a distance $2d_1$ from the beam waist. They are

$$(M_2)_{mn} = \delta_{mn} \, \exp[-i \, 2m \, \tan^{-1}(4d_1/kw_o{}^2)] \qquad (A4)$$

The elements of M_6 are given by the same expression with d_1 replaced by d_2. We must note here that in order to be consistent with Marcatili and Schmeltzer's [6] convention of assuming that the field in the waveguide goes as $\exp(i\gamma z)$, we have assumed that the free space field contains a factor $\exp(+ikz)$ rather than the usually assumed $\exp(-ikz)$. This entails taking complex conjugates of all other expressions in the free space mode functions, and the phase shifts of the TEM_{m0} modes are opposite to the usually stated values. With this assumption, the phase shift between TEM_{10} and TEM_{00} in propagating in a given direction is of the same sign as that between HE_{12} and HE_{11} in propagating in the same direction, as it should be.

The matrix elements of M_3 (again noting that we have taken the complex conjugate of the usual TEM mode definition) are given by the integrals

$$(M_3)_{mn} = (2/ww_o) \int_0^\infty dr^2 \, L_m(\alpha r^2) \, L_n(\beta r^2) \, \exp(-qr^2) \tag{A5}$$

where

$$\alpha = 2/w_o^2 \tag{A6}$$

$$\beta = 2/w^2 \tag{A7}$$

$$q = \frac{1}{w_o^2} + \frac{1}{w^2} - i\frac{k}{2R} \tag{A8}$$

$$w = w_o \left[1 + (4d_1/kw_o^2)^2 \right]^{\frac{1}{2}} \tag{A9}$$

$$R = 2d_1 \left[1 + (kw_o^2/4d_1)^2 \right] \tag{A10}$$

The integral in Equation (A5) is a special case of the type considered by Kogelnik [12], who found that it can be evaluated analytically, with the result

$$(M_3)_{mn} = \frac{2}{ww_o q} \frac{(m+n)!}{m!\, n!} \left(1 - \frac{\alpha}{q}\right)^m \left(1 - \frac{\beta}{q}\right)^n F(-m,-n,-m-n;x) \qquad (A11)$$

where F is the hypergeometric function and

$$x = \frac{q(q - \alpha - \beta)}{(q - \alpha)(q - \beta)} \qquad (A12)$$

If we make use of Equations (A6-A10), we find that x simplifies to

$$x = 1 + (kw_o^2/2d_1)^2 \qquad (A13)$$

After considerable algebra the expression for the matrix element simplifies to

$$(M_3)_{mn} = \frac{(m+n)!}{m!\, n!} (x-1)^{\frac{1}{2}} x^{-(m+n+1)/2} F(-m,-n,-m-n;x) \exp[i(\phi_1 + m\phi_2 + n\phi_3)] \qquad (A14)$$

where

$$\phi_1 = \tan^{-1}[(x-1)^{\frac{1}{2}}/(x+1)] \qquad (A15)$$

$$\phi_2 = \pi + \tan^{-1}[(x-1)^{\frac{1}{2}}] \qquad (A16)$$

$$\phi_3 = -\tan^{-1}[(x-1)^{3/2}/(3x+1)] \qquad (A17)$$

The elements of M_7 are given by the same expression, but with d_1 replaced by d_2 in Equation (A13). We note that the hypergeometric function F is a polynomial in x whose degree is the smaller of the two integers m and n. As d_1 goes to zero, x, and hence F, become infinite, while the remainder of the expression for $(M_3)_{mn}$ goes to zero. The net effect is cancellation, so that as d_1 goes to zero, M_3 approaches the identity matrix. The computer, however, does not recognize this cancellation, and therefore must be told explicitly to set M_3 or M_7 equal to the identity matrix whenever d_1 or d_2, respectively, is zero.

Finally, the diagonal matrix M_5 is given by

$$(M_5)_{mn} = \delta_{mn} \exp[-u_{1m}{}^2 \,(\ell/ka^2)\,(\mathrm{Re}\ \nu_n/ka)]$$
$$\times \exp[-\tfrac{i}{2}\,(u_{1m}{}^2 - u_{11}{}^2)\,(\ell/ka^2)\,(1 + 2\ \mathrm{Im}\ \nu_n/ka)] \qquad (A18)$$

where, again, we have considered only the relative phase shift between the

HE_{1m} and HE_{11} modes.

References

[1] A third configuration often discussed in theoretical papers, but rarely used in practice, consists of long radius of curvature mirrors placed far from the ends of the waveguide.

[2] R. L. Abrams, "Coupling Losses in Hollow Waveguide Laser Resonators," IEEE J. Quant. Elect., vol. QE-8, pp. 838-843, Nov. 1972.

[3] J. J. Degnan and D. R. Hall, "Finite-Aperture Waveguide-Laser Resonator," IEEE J. Quant. Elect., vol. QE-9, pp. 901-910, Sept. 1973.

[4] R. E. Jensen and M. S. Tobin, "CO_2 Waveguide Gas Laser," Appl. Phys. Lett., vol. 20, pp. 508-510, 15 June 1972.

[5] R. Gerlach and N. M. Amer, "Novel CO_2/N_2O Waveguide Laser," Rev. Sci. Instr., vol. 50, pp. 1539-1541, Dec. 1979.

[6] E. A. J. Marcatili and R. A. Schmeltzer, "Hollow Metallic and Dielectric Waveguides for Long Distance Optical Transmission and Lasers," Bell Syst. Tech. J., vol. 43, pp. 1783-1809, July 1964. The modes designated EH_{nm} in this reference are herein designated HE_{nm}, in keeping with the greater part of the waveguide literature.

[7] A. N. Chester and R. L. Abrams, "Mode Losses in Hollow-Waveguide Lasers," Appl. Phys. Lett., vol. 21, pp. 576-578, 15 Dec. 1972.

[8] R. L. Abrams and A. N. Chester, "Resonator Theory for Hollow Waveguide Lasers," Appl. Opt., vol. 13, pp. 2117-2125, Sept. 1974.

[9] F. P. Roullard, III, and M. Bass, "Transverse Mode Control in High Gain, Millimeter Bore, Waveguide Lasers," IEEE J. of Quant. Elect., vol. QE-13, pp. 813-819, Oct. 1977.

[10] M. Lyszyk, F. Herlemont and J. Lemaire, "A Waveguide CO_2 Laser Operating in a Gaussian Mode: Experimental Analysis," Opt. Commun., vol. 36, pp.

327-330, 15 Feb. 1981.

[11] H. Kogelnik and T. Li, "Laser Beams and Resonators," Proc. IEEE, vol. 54, pp. 1312-1329, Oct. 1966.

[12] H. Kogelnik, "Coupling and Conversion Coefficients for Optical Modes," in J. Fox, ed., Proc. Symp. Quasi-Optics, New York, 1964, pp. 333-347 (Polytechnic Press, Brooklyn, 1964).

[13] See for example A. L. S. Smith and S. Moffatt, "Opto-Galvanic Stabilized CO_2 Laser," Opt. Commun., vol. 30, pp. 213-218, Aug. 1979.

[14] M. Tacke, "The Influence of Losses of Hollow Dielectric Waveguides on the Mode Shape," IEEE J. Quant. Elect., vol. QE-18, pp. 2022-2026, Dec. 1982.

[15] H. G. Häfele, "Das Infrarotspektrum des Rubins," Z. Naturforsch., vol. 18a, pp. 331-335, Mar. 1963.

[16] M. G. Lang and W. L. Wolfe, "Optical Constants of Fused Silica and Sapphire from 0.3 to 25 μm," Appl. Opt., vol. 22, pp. 1267-1268, 1 May 1983; erratum vol. 22, p. 2949, 1 Oct. 1983.

[17] R. L. Abrams and W. B. Bridges, "Characteristics of Sealed-Off Waveguide CO_2 Lasers," IEEE J. Quant. Elect., vol. QE-9, pp. 940-946, Sept. 1973.

[18] D. R. Hall, E. K. Gorton, and R. M. Jenkins, "10-μm Propagation Losses in Hollow Dielectric Waveguides," J. Appl. Phys., vol. 48, pp. 1212-1216, Mar. 1977.

[19] J. P. Crenn, "Optical Theory of Gaussian Beam Transmission through a Hollow Circular Dielectric Waveguide," Appl. Opt., vol. 21, pp. 4533-4541, 15 Dec. 1982; erratum vol. 22, p. 1426, 15 May 1983.

[20] R. Gerlach, D. Wei, and N. M. Amer, "A Computer Program for Calculation of Resonator Losses for Waveguide Lasers Using Flat Mirrors," LBL-16945,

1984, available from Technical Information Center, Lawrence Berkeley

Laboratory, Berkeley, CA. 94720.

[21] W. Magnus, F. Oberhettiger and R. P. Soni, Formulas and Theorems for

the Special Functions of Mathematical Physics, pp. 239-249, (Springer-

Verlag, New York, 1966).

TABLE I. Values of the material parameter ν_n for alumina at CO_2 laser wavelengths.[a]

CO_2 Laser Transition	Wavelength (μm)	Re ν_n			Im ν_n		
		$E \perp c$	$E \parallel c$	Avg.[b]	$E \perp c$	$E \parallel c$	Avg.[b]
10P(20)	10.588	0.16	0.11	0.14	−1.14	−1.05	−1.11
10R(20)	10.244	2.09	0.28	1.49	−0.29	−1.95	−0.84
9P(20)	9.549	1.58	2.18	1.78	−0.03	−0.13	−0.06
9R(20)	9.268	1.55	1.90	1.67	−0.02	−0.05	−0.03

[a] Based on the refractive index data of Häfele [15].

[b] Weighted average over crystal orientation, $(2/3)\nu_{n\perp} + (1/3)\nu_{n\parallel}$.

Figure Captions

1. (a) Cavity configuration. Mirror apertures in experiment are 25 mm, but are considered infinite in theoretical analysis.

   (b) Equivalent extended periodic system analyzed theoretically. For explanation of M_1, M_2, etc., see text.

2. Experimentally observed dependence of output power on d_2 for various values of d_1, for a CO_2 laser with a=1.217 mm, ℓ=28 cm.

3. (a) Loss contour plot in d_2/ka^2 vs. d_1/ka^2 plane, for one particular waveguide length, calculated using two waveguide modes. Heavy solid curve is the curve along which $\partial\mathcal{L}/\partial d_2$=0, while heavy dashed curve is that along which $\partial\mathcal{L}/\partial d_1$=0.

   (b) Curves analogous to the heavy solid curve in (a) for various values of the waveguide length parameter ℓ'/ka^2, all calculated using two waveguide modes and with Re ν_n/ka=0.

4. (a) Loss vs. waveguide length for symmetric cavity with various mirror distances $d(=d_1=d_2)$, calculated using two waveguide modes. The top scale, $a^2/\ell'\lambda$, is approximately equal to the waveguide Fresnel number, $a^2/\ell\lambda$.

   (b) Effect of cavity asymmetry on the length dependence of the loss calculated using two modes.

5. (a) Loss vs. waveguide length for lowest-loss mode of symmetric resonator, calculated using one, two, and three waveguide modes.

   (b) Losses vs. length for all three resonator mode solutions found by using three waveguide modes, again for d/ka^2=0.04.

6. Contour plot of losses vs. waveguide length and mirror distance for symmetric cavity, calculated using two waveguide modes. Heavy solid curve is that along which $\partial\mathcal{L}/\partial\ell'$=0, while along heavy dashed curve,

$\partial\mathcal{L}/\partial d=0$.

7. (a) Graph for selecting optimum total cavity length of symmetric reso-
   nator given mirror distance d, for various values of Re ν_n/ka, calculated
   using three waveguide modes. Effective total cavity length L' is nearly
   identical to actual cavity length L; see Equations (6) and (8).

   (b) Minimum cavity loss achieved by using part (a) to select cavity
   length. For comparison, dashed curve represents coupling losses calcu-
   lated from pure-HE_{11} model.

8. (a) Graph for selecting optimum total cavity length of symmetric resona-
   tor given waveguide length ℓ, for various Re ν_n/ka, calculated using
   three waveguide modes.

   (b) Minimum loss achieved by using part (a) to select cavity length.

9. Experimental values of d_2 vs. d_1 for which $\partial\mathcal{L}/\partial d_2=0$, for two lasers of
   different waveguide dimensions. Upper solid curve is three-mode theoret-
   ical curve for larger laser (circular experimental points) while lower
   curve is for smaller laser (square points).

10. Experimental values of ℓ vs. d for which $\partial\mathcal{L}/\partial\ell=0$ (triangles) or $\partial\mathcal{L}/\partial d=0$
    (circles) for symmetric resonator. Solid curve is 3-mode theoretical
    curve for $\partial\mathcal{L}/\partial\ell=0$, while dashed curve is theoretical curve for $\partial\mathcal{L}/\partial d=0$.
    Insets: Examples of experimental graphs of power vs. d at constant ℓ,
    and power vs. ℓ at constant d, from which the points in the main graph
    were obtained.

11. (a) Output power and observed lasing band and branch as a function of
    d_2 for fixed d_1, exhibiting the wavelength selection capabilities of
    the resonator. No determination of the lasing transitions was made
    in the interval 9.3 to 10.3 cm.

(b) Output power vs. mirror distance d_2 at four different wavelengths for a grating-tuned laser with fixed grating distance d_1, exhibiting shift in optimum total cavity length with wavelength.

(a)
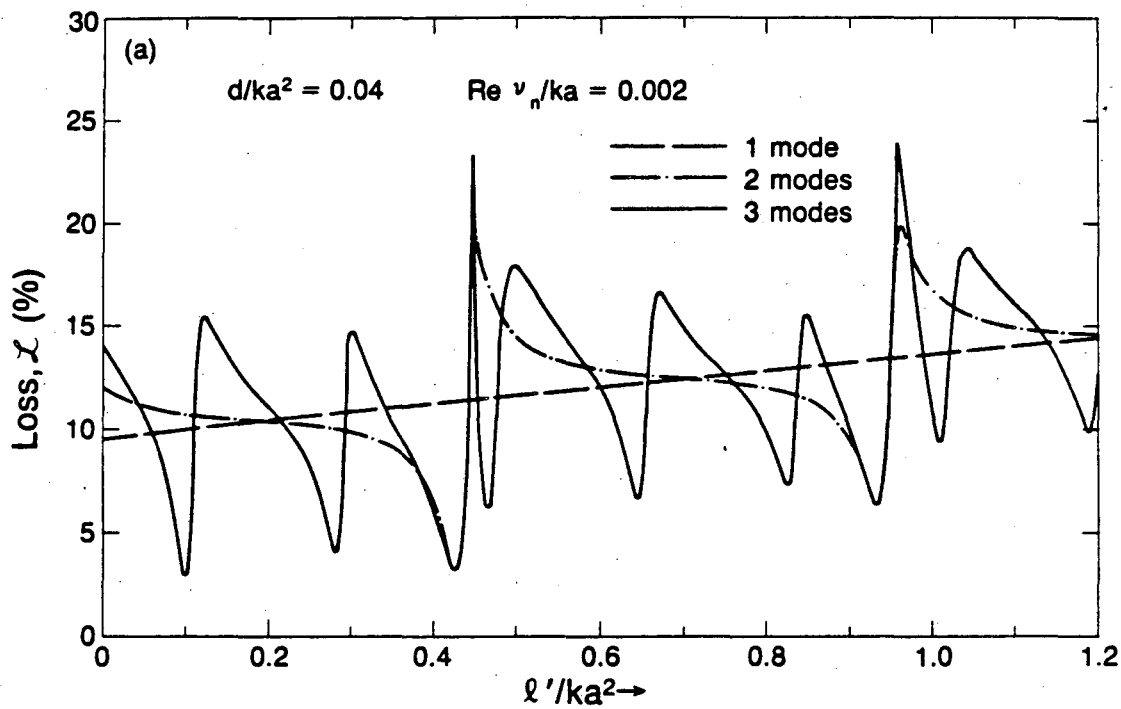

(b)
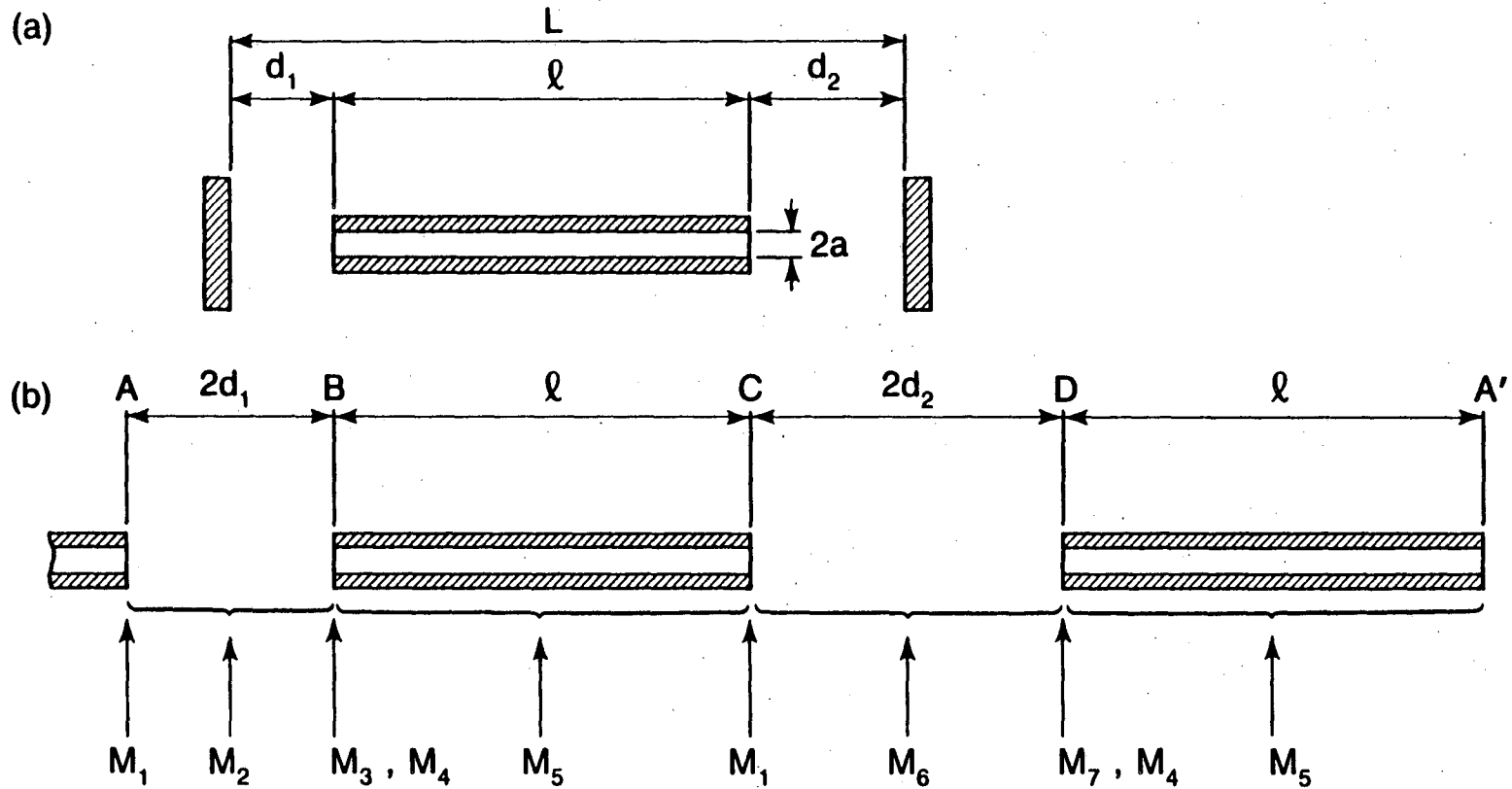
XBL 8310-3358

Figure 1.
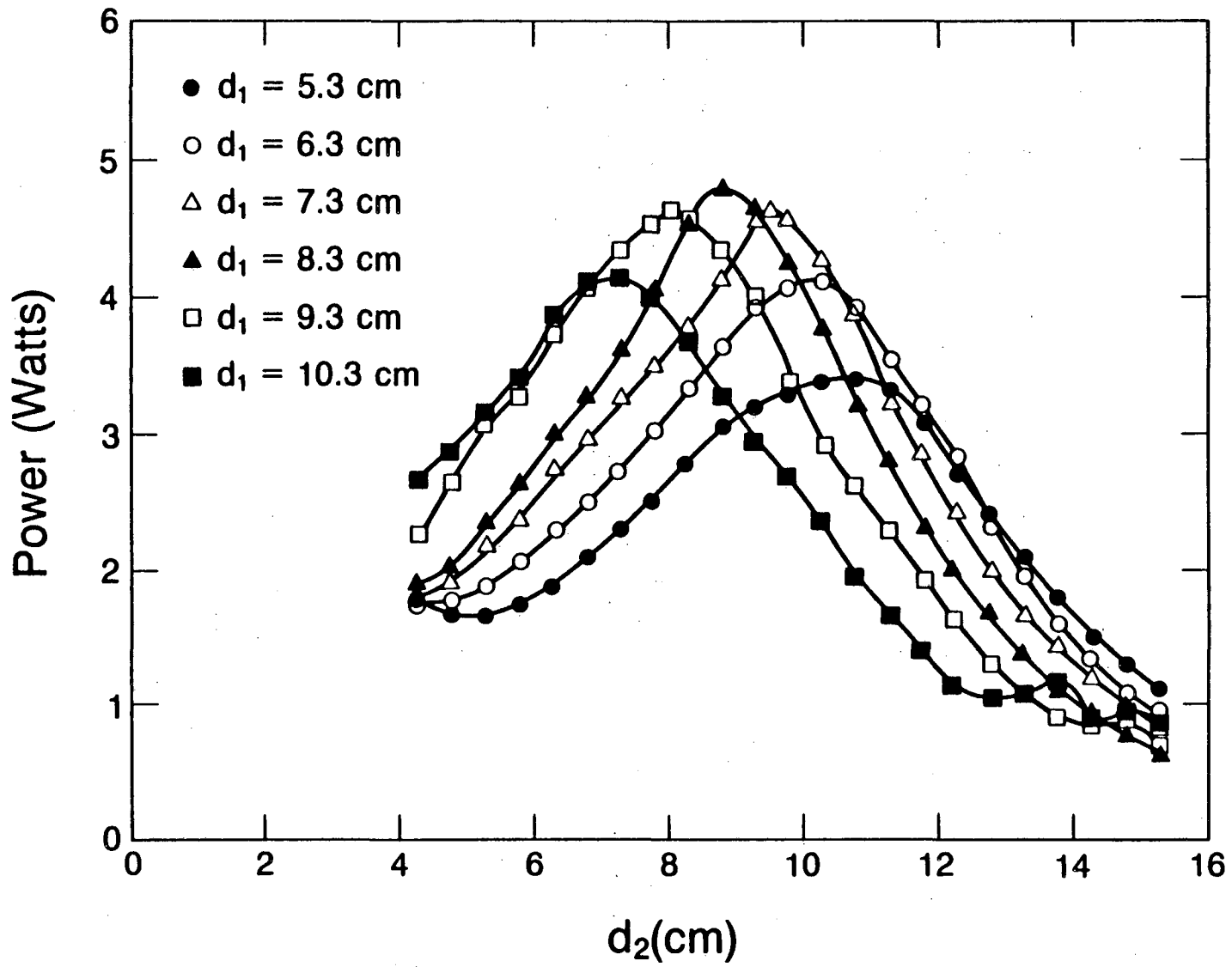
Figure 2.
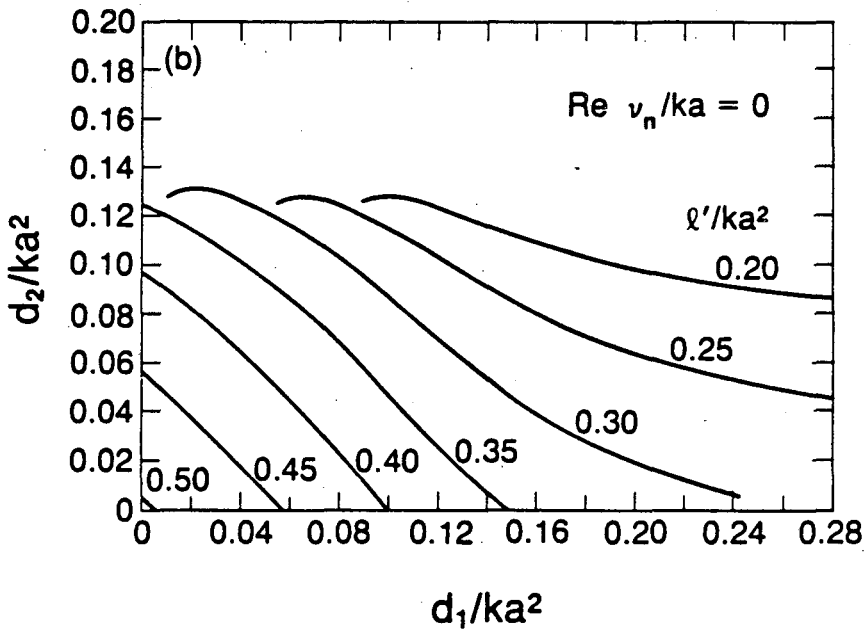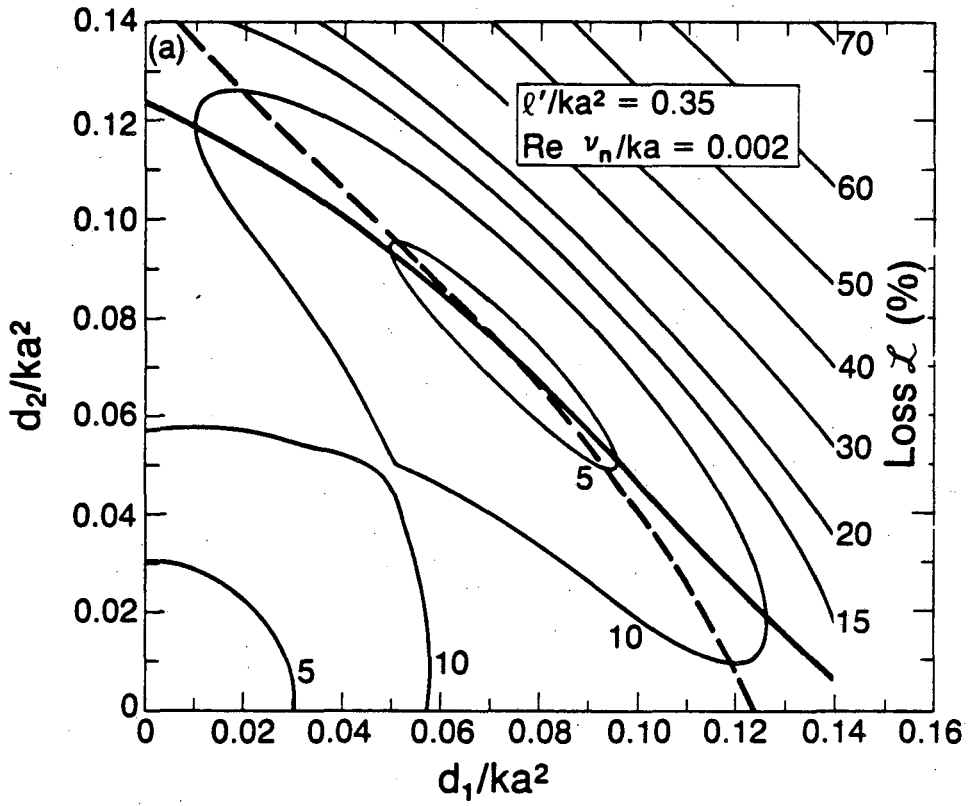
Figure 3.

XBL 8310-3363

Figure 4.
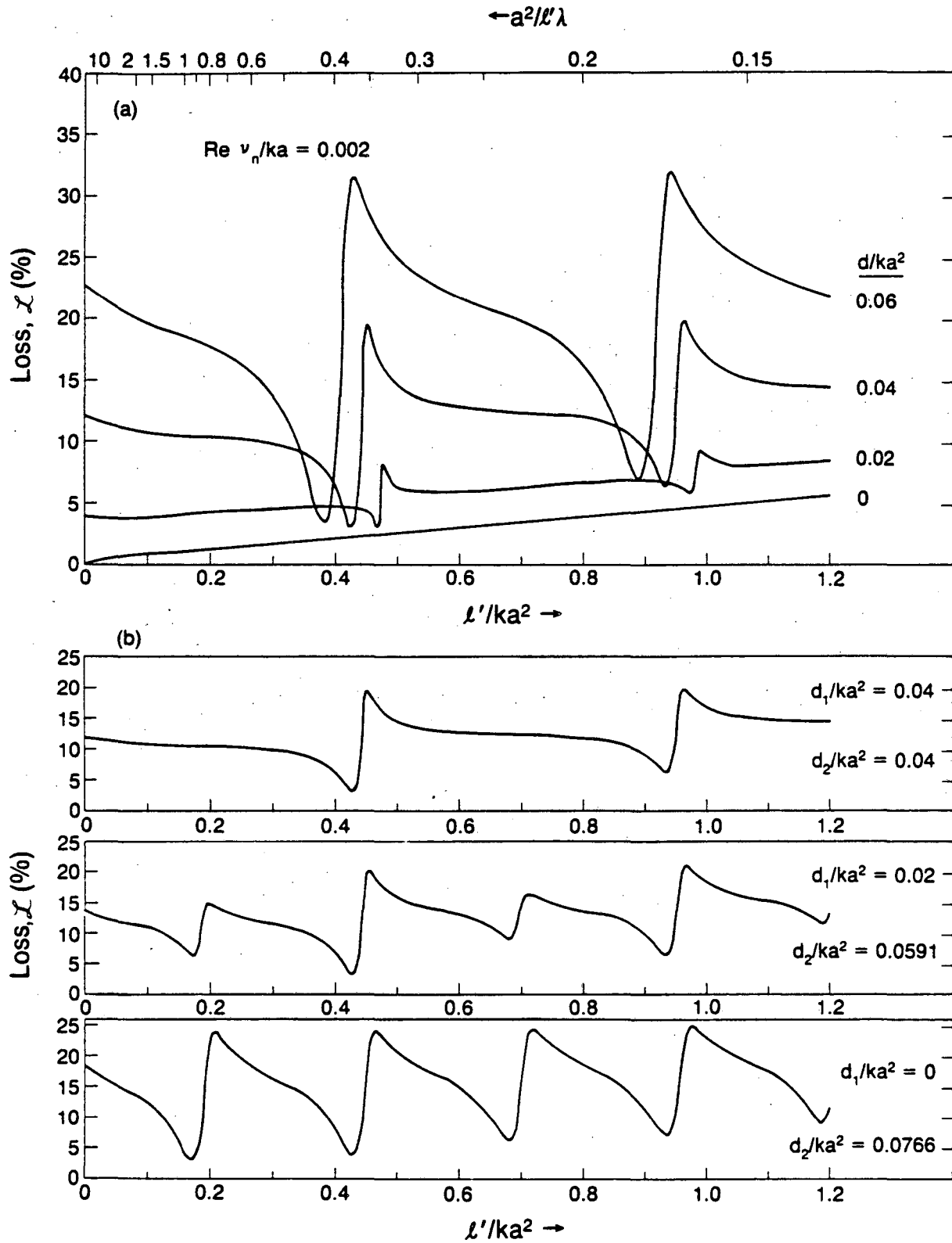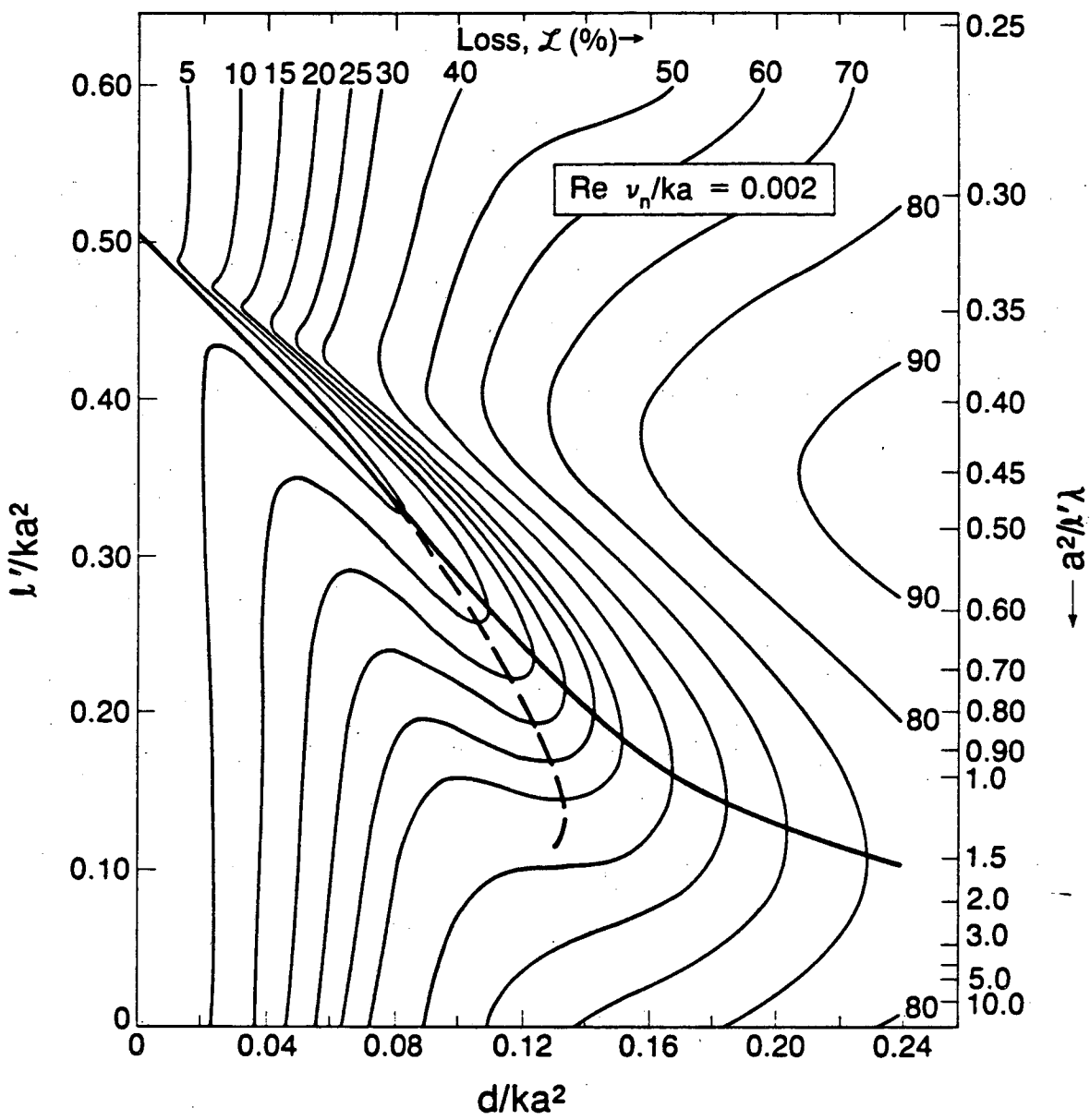
XBL 8310-3359

Figure 5.
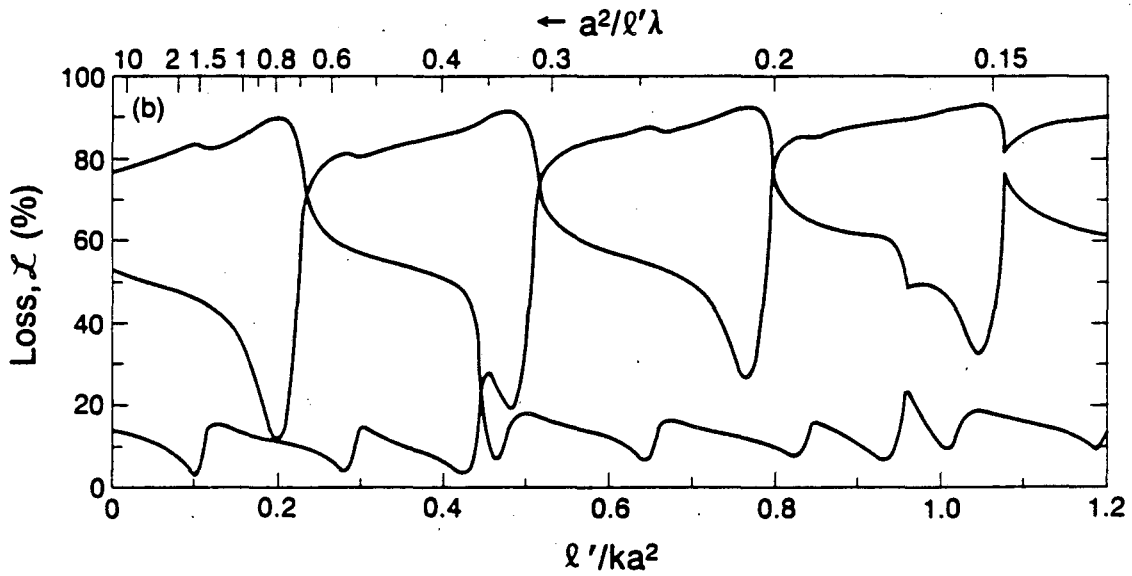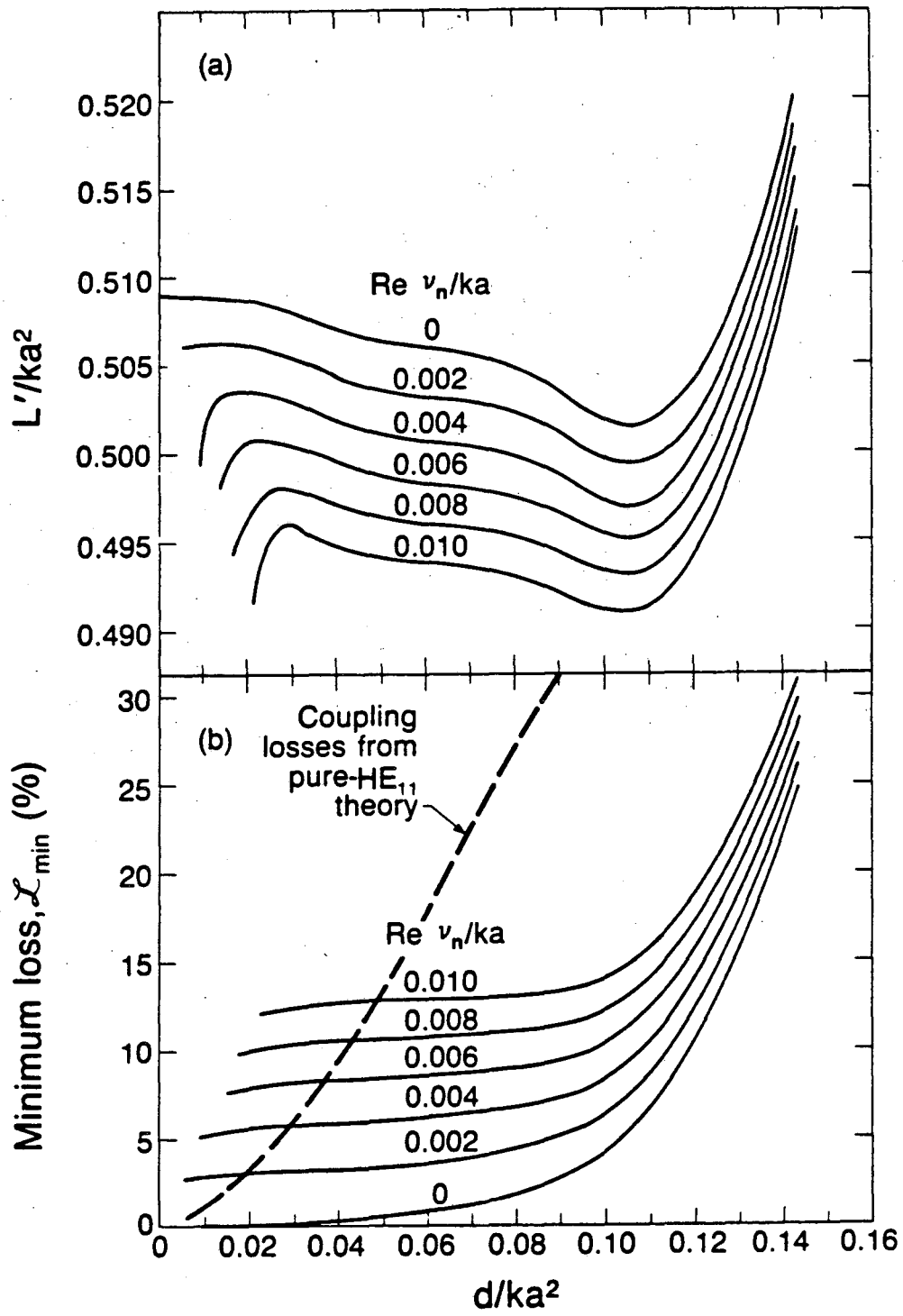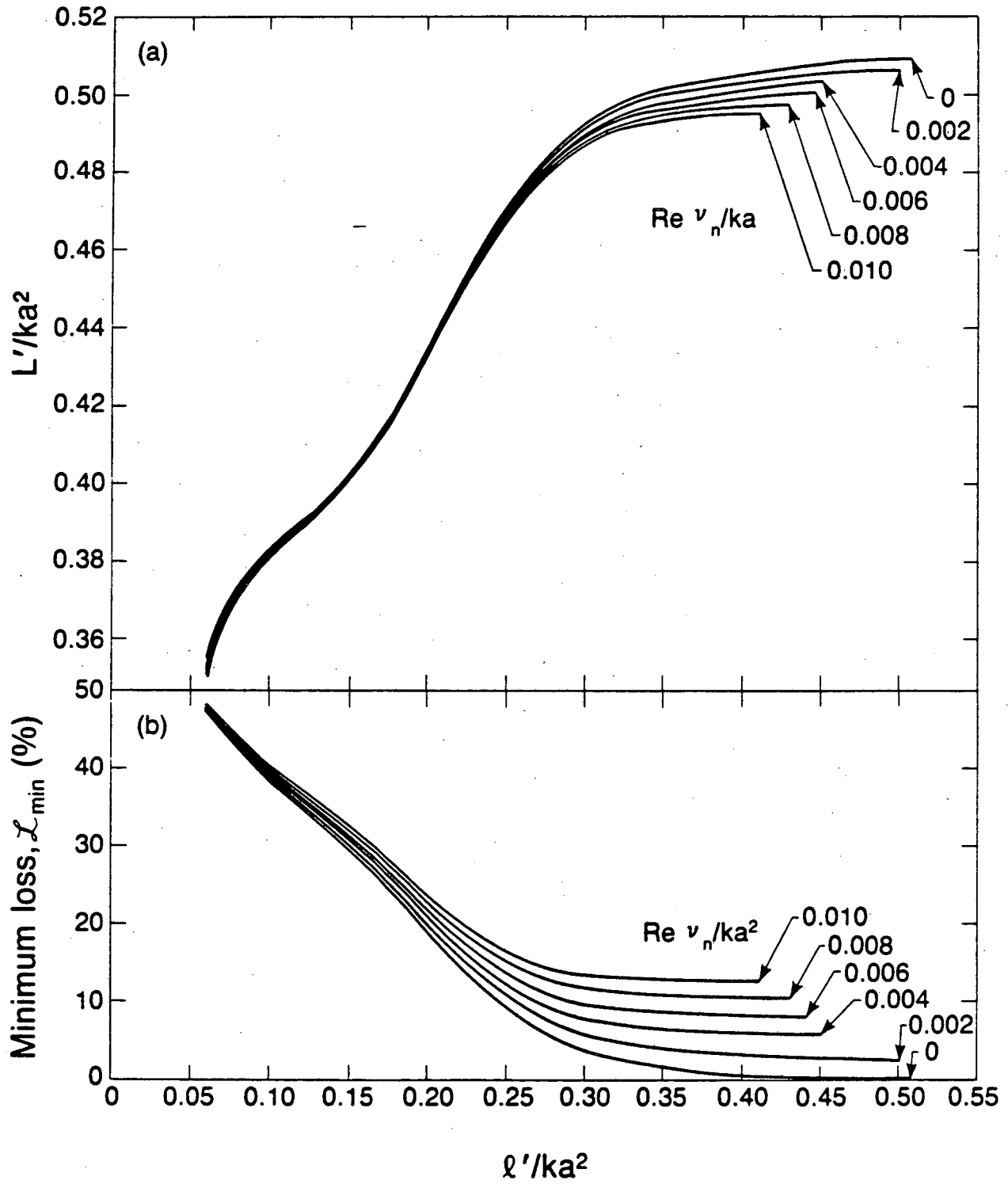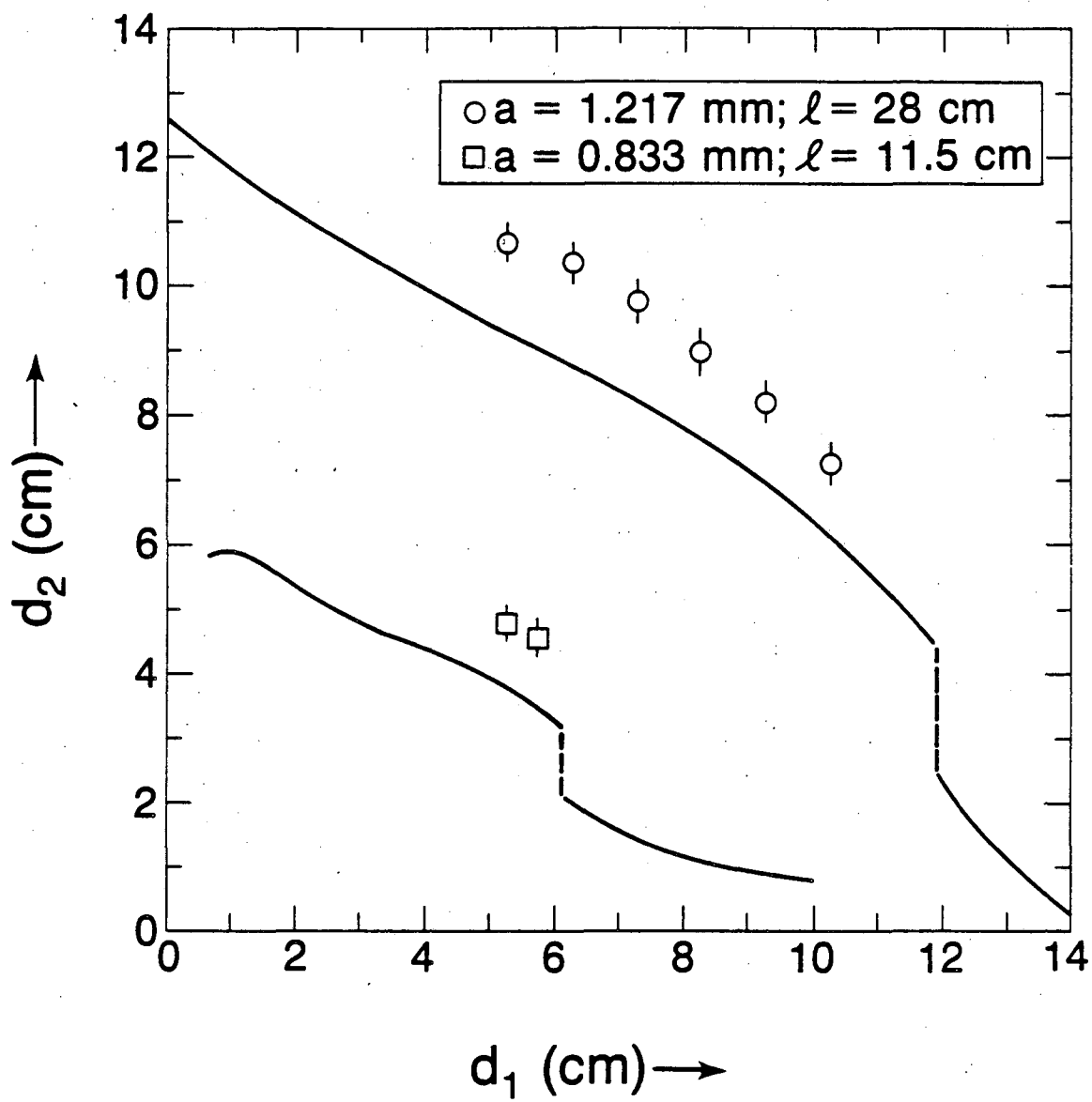
XBL 8311-4527

Figure 6.

XBL 8310-3357

XBL 8310-3361

Figure 7.

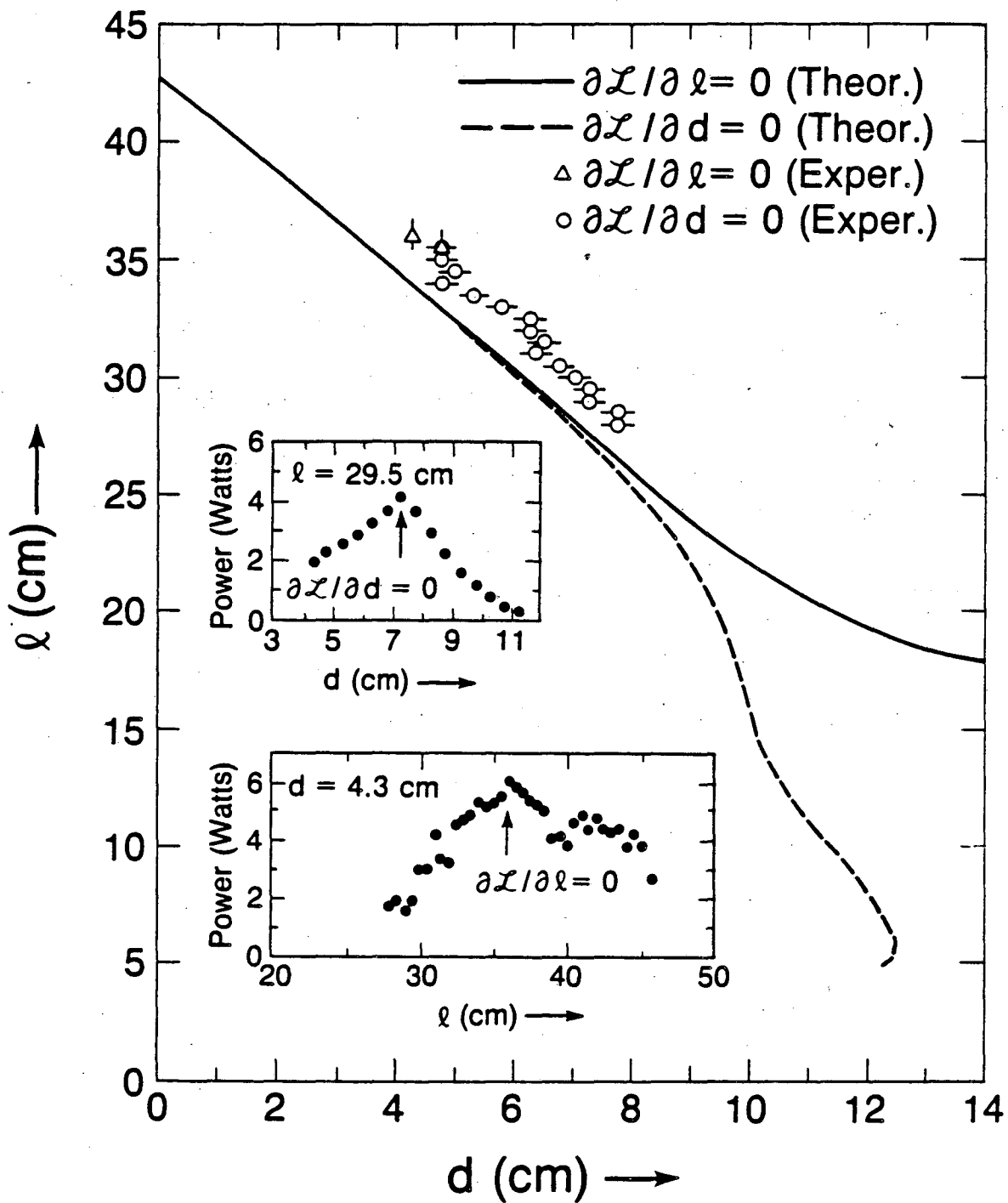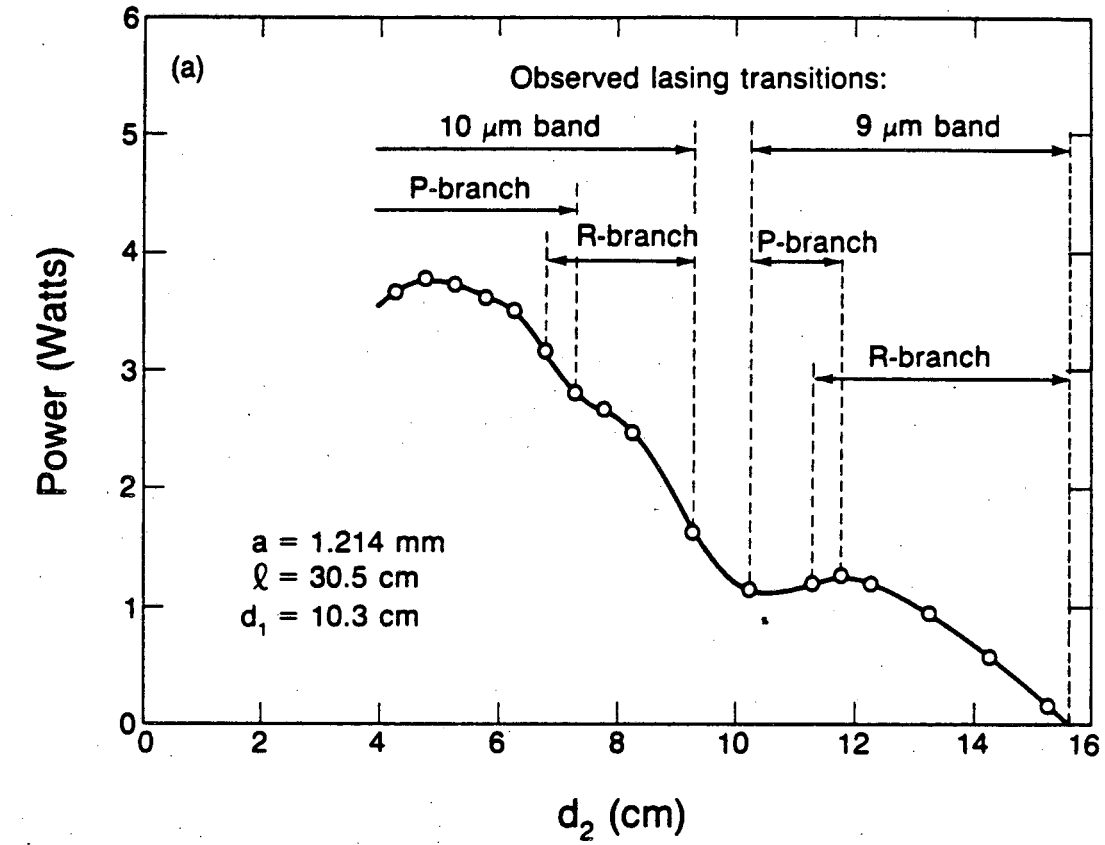Figure 8.

Figure 9.

XBL 8311-4019

Figure 10.

Figure 11.